CHALMERS
UNIVERSITY OF TECHNOLOGY

Energy Optimized Adaptive Cruise Control for Battery Electric Vehicles

Master's thesis in Systems, Control and Mechatronics

HANNES BOLMSTEDT, OTTILIA WAHLGREN

Department of Electrical Engineering
CHALMERS UNIVERSITY OF TECHNOLOGY
Gothenburg, Sweden 2019

Master's thesis 2019

Energy Optimized Adaptive Cruise Control for Battery Electric Vehicles

Using Dynamic Programming

In collaboration with

Volvo Cars

HANNES BOLMSTEDT, OTTILIA WAHLGREN

CHALMERS
UNIVERSITY OF TECHNOLOGY

Department of Electrical Engineering
Chalmers University of Technology
Gothenburg, Sweden 2019

Energy Optimized Adaptive Cruise Control for Battery Electric Vehicles
Using Dynamic Programming
HANNES BOLMSTEDT, OTTILIA WAHLGREN

Supervisors:
Rickard Arvidsson - Director at Propulsion System, Volvo Cars
Fredrik Björkqvist - Team Manager for Virtual Car at Active Safety &
Autonomous Drive, Volvo Cars

Examiner: Tomas McKelvey - Full Professor, Deputy Head of Department, Electrical Engineering

Master's Thesis 2019
Department of Electrical Engineering
Chalmers University of Technology
SE-412 96 Gothenburg
Telephone +46 31 772 1000

Typeset in LaTeX
Gothenburg, Sweden 2019

Energy Optimized Adaptive Cruise Control for Battery Electric Vehicles
Using Dynamic Programming
HANNES BOLMSTEDT, OTTILIA WAHLGREN
Department of Electrical Engineering
Chalmers University of Technology

Abstract

In recent years, a global trend towards more sustainable and autonomous transportation has been changing the car industry. Electrification is on the rise, and Volvo Cars has set out to be a leader with the bold goal of having half of the vehicles sold to be fully electrical by 2025. With more electric vehicles and better autonomous functionality than ever before, it is a natural step to look into energy optimization of the autonomous driving behavior.

The adaptive cruise control (ACC) is responsible for a large portion of driven kilometers in new vehicles. Therefore, this thesis aims to examine the potential of energy optimizing the ACC behavior. To limit the scope, only deceleration scenarios were considered where the vehicle with ACC closes in on a vehicle with constant velocity in front. Two different initial velocities of the vehicle with ACC were tested, while the vehicle in front had the same velocity in both cases. Different time constraints and initial relative distances were tested. All tests were performed in a simulation environment based on Matlab and Simulink, where the power of the electric motors could be measured.

The optimization problem was solved using dynamic programming implemented in Matlab. The solutions derived from the dynamic programming were in the form of vehicle trajectories which were then tested on an electric vehicle model in Simulink. The measured power on the motors could then be compared to that of a traditional ACC. The results show that given the exact same initial and final position and velocity, as well as the same time to travel between the two, an energy optimized solution can decrease the energy usage up to 2.1 % compared to a traditional ACC. Given longer time to reach the goal, while not allowed to react earlier, the energy can be decreased by up to 5.5 %. If instead, the ACC is allowed to react earlier and the trajectory is energy optimized, the energy can be decreased by up to 39.1 %. Note that reacting earlier does not necessarily mean increasing the radar distance, but rather utilizing the information earlier.

Keywords: Adaptive cruise control, dynamic programming, Bellman-Ford algorithm, directed graph, shortest path algorithm, optimization control problem, energy usage, battery electric vehicles, simulation environment.

Acknowledgements

This master thesis is a project written as a collaboration between the department of Electrical Engineering at Chalmers University of Technology and the department of Active Safety at Volvo Cars during the spring of 2019.

First, we would like to thank our supervisors who have always supported and inspired us throughout countless discussions. Their supportive presence and their focus on our interests and opinions has laid the foundation for this project. We have been lucky to have two supervisors from Volvo Cars, Rickard Arvidsson and Fredrik Björkqvist who have shown great interest in our project and who initially introduced us to this project. Our full gratitude also goes to Tomas McKelvey, our supervisor at Chalmers, who has given us invaluable support by answering all our questions and giving us academic guidance. We are very grateful for all the support and time from our supervisors.

We would also like to thank the people at Volvo Cars who have always had time to help us throughout the project. This project is a team effort and would not have been possible without their unconditional help. An extra thank you to Martin Sivertsson who has challenged us with his critical thinking and been a great support for us regarding technical questions. Other special mentions are deserved by Goksan Isil and Mikael Andersson who have taught us how to use the simulation tools and always been available for support and questions. Additionally, we would like to show our gratitude towards Abhishek Bhat, Melih Guldogus and Jingxiong Liu for helping us with all the aspects regarding battery electric vehicles in simulation. Lastly, our thanks to the ACC team at Volvo Cars who helped us find scenarios to test and evaluate the results.

Finally, we want to thank the whole team at Volvo Cars for creating the great work environment that have given us a wonderful experience. You have all been a motivation for us to work hard and to strive for great results.

Hannes Bolmstedt and Ottilia Wahlgren. Gothenburg, June 2019

Contents

List of Abbreviations

ACC	Adaptive Cruise Control
BEV	Battery Electric Vehicle
DP	Dynamic Programming
EOACC	Energy Optimized ACC
OCP	Optimal Control Problem
SOC	State of Charge
SPAS	Simulation Platform for Active Safety
VCC	Volvo Car Corporation

List of Figures

List of Tables

1

Introduction

This chapter introduces the underlying reasons for this project and puts it into a larger perspective. The overall purpose is presented, and boundaries are set up to make the results achievable.

1.1 Background

The transportation sector is responsible for a large portion of humanities greenhouse gas emissions [1]. With better battery technology available and more focus on sustainability in society in general, a global trend towards more and better electric transportation has started. Volvo Cars has announced that by 2025, half of all the sold cars will be fully electrical [2]. However, even for electric vehicles, minimizing the consumption, or in this case the energy usage is crucial with the main reason being the current limitations in battery technology. Historically the range and the charging times has been what has held back electric vehicles the most. Furthermore, most of the electricity produced worldwide is not from renewable sources which further motivates the importance of energy efficiency in the electric vehicles.

Even though emissions from exhaust-related sources are reduced by introducing electric vehicles, the non-exhaust traffic-related sources are estimated to be almost equally responsible for the total traffic-related PM_{10} emissions. PM_{10} is a measurement of mass of particles in the air that have a diameter less than 10 μm. These non-exhaust traffic-related sources are mainly caused by brake wear where urban environments are the most exposed. Dust from brakes are not only unwanted but can also cause health issues for humans as all particles are involved in the respiratory function [3]. Due to these facts, friction braking should always be avoided as it contribute the most to brake wear and wasted energy to heat. Hence, coasting or regenerative breaking is preferred.

Another goal of Volvo Cars is to make cars fully autonomous. There are many reasons for this regarding everything from safety to comfort and traffic flow efficiency. However, letting the car itself control how it is driven also enables the possibility to optimize the driving behavior in regard to energy efficiency and fuel consumption, essentially making the car a perfect eco-driver.

This thesis looks into one of the active safety functions, adaptive cruise control (ACC), which is a system that regulates the speed and acceleration of the car based on the current traffic situation [4]. This function is also a crucial step in making the car autonomous which also includes making the car more efficient in regard to its consumption. A target speed for the ACC is selected by the driver as well as a desired time interval to the vehicle in front.

1.2 Purpose

The primary purpose of this project is to make electric vehicles more efficient. The purpose should be attained by showing the potential of designing an ACC with better energy efficiency than traditional ACC implementations, without compromising safety and with as little compromise to comfort and time as possible. The goal is to show that the traditional ACC function is not optimal with regard to neither liquid fuel nor electric power. The purpose is therefore to examine whether it is worthwhile to optimize ACC functionality. The research is necessary to make electric vehicles more attractive for the market in general and to make transportation more sustainable in particular.

1.3 Boundaries

The development, testing, and verification will be performed in a simulation environment based on Matlab and Simulink. To reduce complexity, it is useful to assess the fidelity required for the specific use case, i.e. fidelity driven simulation. For our purpose, low fidelity traffic models will be used as objects surrounding the host vehicles do not require realistic dynamics and human behavior. The behavior of surrounding objects can therefore be predefined exactly.

The host vehicle has a predefined trajectory, but in contrast to the other objects it has additional functionality and dynamics which will affect its behavior. For this purpose, the main functionality will be an ACC which will adapt the speed and acceleration of the host vehicle to the other objects in the simulation. To limit the computational load and also to simplify the analysis of the output, the host vehicle will not act from other active safety functions such as auto brake, in-lane, or pilot-assist.

In the simulation, consistent conditions can be achieved while in reality, fog, darkness, bad lane markings etc. might affect the results. While some factors can be changed in the simulation environment, e.g. road friction, and disturbances could be added to the sensor signals, we will for simplicity only test with *perfect conditions*.

A specific scenario will be chosen for which we will energy optimize the behavior of the host vehicle. This scenario will focus on the deceleration phase. As a result, the

developed model to optimize the behavior might not work in all situations. Special use cases such as curves or mis-use cases such as roundabouts and intersections will not be taken into consideration. The simulated scenario is chosen to correspond to realistic traffic situations as much as possible.

2

Theory

In the sections below, different parts of the theory will be presented. The theory is later used to develop the algorithm to optimize the energy usage.

This chapter will introduce the theory behind adaptive cruise control as well as the technology of regenerative braking. Furthermore, the modelling of a battery electric vehicle is described which is the basis for developing a cost function. Lastly, the theory of dynamic programming as well as the simulation environment is presented.

2.1 Adaptive Cruise Control

Adaptive cruise control (ACC) is a common system in newer cars that adapts the vehicle speed relative to other vehicles in front to maintain a safe distance. The vehicle uses sensor information, commonly radar and cameras to detect vehicles and other objects such as pedestrians or cyclists [4].

An ACC usually has two different control modes. A speed control mode and a distance control mode. The speed control mode is used when there is no detected vehicle ahead. For these cases, a set speed determined by the driver is used as reference. The vehicle will keep the set speed until it detects another vehicle. The set speed can easily be increased or decreased by the driver.

The second mode is the distance control mode which is active when another vehicle is present in front. It is necessary to keep a minimum safety distance, however the driver can choose to increase the minimum distance. The minimum distance is commonly defined as a time gap rather than a distance gap since what is considered a safe distance varies with speed. The time gap determined by the driver is used by the ACC and will be kept until the vehicle in front accelerates beyond the set speed or switches lane. The speed control mode would then take over and control the vehicle. This is illustrated in Figure 2.1.

On Volvo Cars, ACC and pilot assist are two separate systems that can be active simultaneously. While the ACC regulated the speed, the pilot assist controls the steering.

There is an ISO standard regarding ACC systems including performance requirements and test procedures [5]. The performance requirements include no deceleration sharper than 3.5 m/s^2 except in emergencies, and no acceleration sharper than 2 m/s^2.

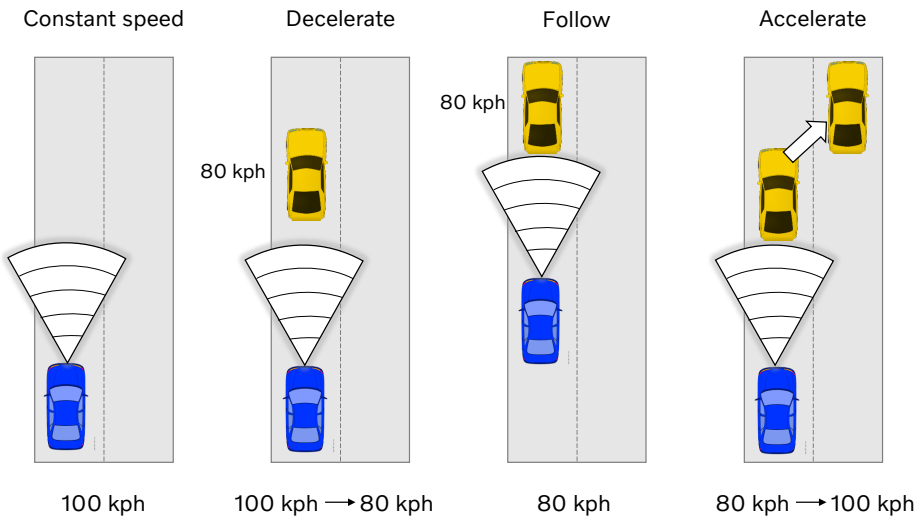

Figure 2.1: Vehicle using ACC with a set speed of 100 kph

2.2 Regenerative Braking

This section describes the technology of the regenerating energy in battery electric vehicles (BEV) and its advantages not only in an energy point of view but also in an environmental point of view.

The battery is the power source for BEV:s which provides the motors with electric energy. The energy is used by the motors in order to rotate the wheels and produce kinetic energy. For conventional vehicles, this kinetic energy is wasted to heat energy when the vehicle is braking due to friction on the brake pads. However, for battery electric vehicles, the motor can act as a generator providing enough resistance to slow the vehicle down. This enables the motor to convert the kinetic energy to electric energy and store it in the battery. This is called regenerative breaking [6].

The technique is used in BEV:s to extend their driving range. This in contrast to the conventional braking system where the kinetic energy is converted to heat which is both unwanted and wasted. In addition, studies have shown that wear-particles from braking is a major reason for air pollution on the roads [3].

These fine particles are emitted into the air which has shown to have a negative

impact on our health. Even though the total exhaust traffic-related particles are decreasing due to better technology and electric vehicles, the emissions due to braking will not necessarily decrease. Studies has shown that wear-particles from tires can contribute to approximately 55% to the total non-exhaust traffic-related PM_{10} emissions and also 21% to the total exhaust traffic-related PM_{10} emissions in urban environments. These percentages are lower in freeway environments since brakes are used less [3]. PM_{10} is a measure of mass of particles in the air that are less than 10 μm in diameter which is small enough to cause lung diseases when inhaled [7].

The prime chemicals from brake wear are Cu, Fe, Ba, and Pb. They are all impacting the respiratory function and have also been classified as a potential danger to health. Although, there is a lack of studies on this area which makes the relationship between the brake wear and the human health incomplete [3]. By coasting, i.e. rolling without using any power, and by using regenerative brakes instead of friction brakes, the brake wear will be reduced.

2.3 Modelling of a Battery Electric Vehicle

The subsections below describe the dynamics of the vehicle as well as the different systems within the vehicle. The following subsections are used to describe the energy usage for a BEV. The models below are based on state changes where the state variables are

$$x_n = \begin{bmatrix} v_n \\ d_n \end{bmatrix} \tag{2.1}$$

where v_n describes the vehicles velocity at a discrete time step n, and d_n its relative distance between itself and the target vehicle in front.

2.3.1 Motion Equations

In order to derive the motion equations, the time and acceleration required for a state change must be derived from the states themselves. For simplicity, it is assumed that the velocity changes linearly between two states. For a state change between x_0 and x_1 and with a known constant target velocity of v_t, the following equations are used to find the required time and acceleration for a state change.

$$
\begin{aligned}
v_{\text{avg}}(v_0, v_1) &= \frac{v_1 + v_0}{2} \\
\Delta v(v_0, v_1) &= v_{\text{avg}}(v_0, v_1) - v_{\text{t}} \\
\Delta d(d_0, d_1) &= d_0 - d_1 \\
t(v_0, v_1, d_0, d_1) &= \frac{\Delta d(d_0, d_1)}{\Delta v(v_0, v_1)} \\
a(v_0, v_1, d_0, d_1) &= \frac{v_1 - v_0}{t(v_0, v_1, d_0, d_1)}
\end{aligned}
\tag{2.2}
$$

where v_{avg} is the average speed of the host vehicle during the state change, Δv is the average relative velocity with regard to the target vehicle, Δd is the difference in distance in between the states, t is the time required for the state change and a is the acceleration required for the state change. To avoid divisions by zero and negative time, the problem needs constraints. This is described in more detail in section *2.4 Dynamic Programming*.

By Newton's law of motion, the vehicle's longitudinal acceleration can be described as

$$
(m + m_{\text{rotation}}) \cdot a(x_0, x_1) = F_{\text{t}}(x_0, x_1) - F_{\text{drag}}(x_0, x_1) \tag{2.3}
$$

The movement is affected by forces acting on the vehicle's body, where $F_{\text{drag}}(x_0, x_1)$ is the aerodynamic drag force which can be described as

$$
F_{\text{drag}}(x_0, x_1) = \frac{\rho_{\text{a}} \cdot c_{\text{d}} \cdot A \cdot v_{\text{avg}}(v_0, v_1)^2}{2} \tag{2.4}
$$

where ρ_{a}, c_{d}, and A are the air density, the aerodynamic drag coefficient and the cross-sectional area respectively.

The equivalent mass of all the rotational parts due to inertia is notated m_{rotation} and can be described as

$$
m_{\text{rotation}} = \frac{n_{\text{tire}} \cdot j_{\text{tire}} + n_{\text{em}} \cdot j_{\text{em}} + n_{\text{trn}} \cdot j_{\text{trn}}}{r_{\text{tire}}^2} \tag{2.5}
$$

where r_{tire} is the radius of the wheel at 75 kph, n_{tire}, n_{em}, and n_{trn} is the number of wheels, electric motors and transmissions respectively. j_{tire}, j_{em}, and j_{trn} is the inertia of a wheel, an electric motor and a transmission respectively.

With this, equation (2.3) can be used to calculate $F_{\text{t}}(x_0, x_1)$, i.e the body force required from the wheels, to achieve the state change. There is also rolling resistance which has to be taken into account which is dependent on the rotational speed of the wheels as well as other factors such as friction and tires. The angular velocity of the wheels is found by simply dividing the vehicle velocity by the radius of the wheels.

$$\omega_{\mathrm{w}}(x_0, x_1) = \frac{v_{\mathrm{avg}}(v_0, v_1)}{r_{\mathrm{tire}}} \tag{2.6}$$

The rolling resistance torque per wheel, assuming same normal force on all wheels, is then given by

$$T_{\mathrm{r}}(x_0, x_1) = ((a \cdot r_{\mathrm{tire}} \cdot \omega_{\mathrm{w}}(x_0, x_1))^2 \cdot b + c) \cdot r_{\mathrm{tire}} \cdot \frac{m}{n_{\mathrm{tire}}} \cdot g \tag{2.7}$$

where a, b and c are constants related to the tires, friction etc. and g is the gravitational constant. The actual torque required per wheel is then given by

$$T_{\mathrm{w}}(x_0, x_1) = \frac{F_{\mathrm{t}}(x_0, x_1)}{n_{\mathrm{tire}}} \cdot r_{\mathrm{tire}} + T_{\mathrm{r}}(x_0, x_1) \tag{2.8}$$

2.3.2 Transmission Model

The torque requested from the electric motor and the resulting torque on the wheels are related through a transmission ratio, R_{t} and an efficiency $\eta(\omega_{\mathrm{w}}(x_0, x_1), T_{\mathrm{w}}(x_0, x_1))$. Given the torque on the wheels, and assuming the torque is equally distributed between the front and rear electric motor, the electric motor torque, T_{em}, can be calculated as

$$T_{\mathrm{em}}(x_0, x_1) = \frac{n_{\mathrm{em}} \cdot T_{\mathrm{w}}(x_0, x_1)}{\eta(\omega_{\mathrm{w}}(x_0, x_1), T_{\mathrm{w}}(x_0, x_1)) \cdot R_{\mathrm{trn}}} \tag{2.9}$$

The demanded torque, T_{em}, can be either positive or negative. The torque is also limited to its maximum and minimum capacity based on the angular velocity which will constrain the torque demanded on the electric motor.

$$T_{\mathrm{min}} \leq T_{\mathrm{em}} \leq T_{\mathrm{max}} \tag{2.10}$$

2.3.3 Electric Machine Model

Depending on the velocity profile, the electric motor can either consume energy or generate power to the battery. The latter is called recuperation and will depend on the requested torque and the angular velocity of the electric motor, which is related to the angular velocity of the wheels as

$$\omega_{\mathrm{m}}(x_0, x_1) = R_{\mathrm{trn}} \cdot \omega_{\mathrm{w}}(x_0, x_1) \tag{2.11}$$

The mechanical power without losses is then simply calculated as

$$P_{\mathrm{mech}}(x_0, x_1) = T_{\mathrm{em}}(x_0, x_1) \cdot \omega_{\mathrm{m}}(x_0, x_1) \tag{2.12}$$

The losses are given as a function $\xi(\omega_{\mathrm{r}}(x_0, x_1), T_{\mathrm{em}}(x_0, x_1))$, depending on the angular velocity and the torque

$$P_{\mathrm{loss}}(x_0, x_1) = \xi(\omega_{\mathrm{r}}(x_0, x_1), T_{\mathrm{em}}(x_0, x_1)) \tag{2.13}$$

The total required power for one electric motor is then simply the sum of the mechanical power and the total losses.

$$P_{\mathrm{elec}}(x_0, x_1) = P_{\mathrm{mech}}(x_0, x_1) + P_{\mathrm{loss}}(x_0, x_1) \tag{2.14}$$

2.3.4 Battery Model

The battery model would normally include the value of state of charge, SOC, which affect the current, I_{batt}, in the battery. But for the scenarios tested in this thesis, the SOC is assumed to be constant, or at least not vary enough to make a significant difference [8]. A fixed value of the SOC will therefore be used to calculate mean values of the resistance in the battery, R_{batt}, and the open circuit voltage, U_{ocv}. The equation for the current can then be expressed as

$$I_{\mathrm{batt}}(x_0, x_1) = \frac{1}{2 \cdot R_{\mathrm{batt}}}\Big(U_{\mathrm{ocv}} - \sqrt{U_{\mathrm{ocv}}^2 - 4R_{\mathrm{batt}} \cdot P_{\mathrm{elec}}(x_0, x_1)}\Big) \tag{2.15}$$

where R_{batt} is the battery resistance. We can then obtain the inner electrochemical battery power as

$$P_{\mathrm{batt}}(x_0, x_1) = I_{\mathrm{batt}}(x_0, x_1) \cdot \Big(U_{\mathrm{ocv}} - R_{\mathrm{batt}} \cdot I_{\mathrm{batt}}(x_0, x_1)\Big) \tag{2.16}$$

which will depend on the velocity and the torque demanded for that speed. P_{batt} can be either positive or negative and will be negative for when electricity is regenerated and positive when energy is consumed.

2.4 Dynamic Programming

Dynamic Programming (DP) is a method than can be used to solve optimization problems where the basic idea is to break down a complex problem into a reasonable number of overlapping subproblems. This is very beneficial in this case since the problem is highly non-linear in nature. The idea is to later solve each subproblem individually and use those optimal solutions to find an optimal solution to the whole problem. There are many different algorithms that are based on DP, for example the Bellman-Ford algorithm which will later be described in more detail [10].

The optimal control problem (OCP) will be described by a cost function and constraints. The problem will be defined such that the task is to find the admissible

control variable u^* which will result in the system to following an admissible trajectory x^*, i.e. find (x^*, u^*). Given an OCP, an initial state, x_i, and a final state, x_f, we can find the initial and final cost functions, f_{init} and f_{final} respectively. Both will be based on the given cost functions between each state, f_{cost}. The following theory is based on the paper *Discrete Time Optimal Control* by T. McKelvey [9] and *Dynamic Programming and Optimal Control* by DP Bertsekas [10].

The OCP can be formulated as

$$(x^*, u^*) = \arg\min_{x,u} \left\{ f_{\text{init}}(x_1) + f_{\text{final}}(x_N) + \sum_{n=1}^{N-1} f_{\text{cost}}(n, x_n, u_n) \right\} \tag{2.17}$$

where N will be the final step, i.e. $x_{\text{final}} = x_N$. To obtain the optimal solution, it is necessary to define constraints to this OCP.

First of all, the state transition function, f_x, will be the function that describes the next state. The rest of the constraints on the state will be denoted as q. The constraints can be formulated as

$$\begin{aligned} \text{s.t. } & q(n, x_n, u_n) \leq 0 \\ & x_{n+1} = f_x(n, x_n, u_n) \end{aligned} \tag{2.18}$$

At each time n we have feasible state pairs which can be denoted $(x_n, x_{n+1}) \in \mathcal{X}_n$ where $\mathcal{X}_n$ is the feasible set of pairs. If the transmission pair is in that set there will exist a control variable, u_n, that will make sure that all constraints just mentioned are fulfilled. We can then assume that the control variable, u_n, can be described by the function

$$u_n = q_u(n, x_n, x_{n+1}), \qquad (x_n, x_{n+1}) \in \mathcal{X}_n \tag{2.19}$$

which only describes that the constraints are fulfilled. To further simplify the cost function (2.17), we can introduce a new function, f, that will consist of all the constraints on the state and control, q, and the cost function, f_{cost}. f is given by

$$f(n, x_n, x_{n+1}) = \begin{cases} f_{\text{cost}}(n, x_n, q_u(n, x_n, x_{n+1})), & (x_n, x_{n+1}) \in \mathcal{X}_n \\ \infty & (x_n, x_{n+1}) \notin \mathcal{X}_n \end{cases} \tag{2.20}$$

This enables us to express the new OCP as

$$x^* = \arg\min_{x} \left\{ f_{\text{init}}(x_1) + f_{\text{final}}(x_N) + \sum_{n=1}^{N-1} f(n, x_n, x_{n+1}) \right\} \tag{2.21}$$

The solution is then to solve equation (2.21) and the optimal control variable is given by equation (2.19). By that we will obtain the optimal trajectory x^*.

2.4.1 Bellman-Ford Algorithm

The stated equations, (2.21) and (2.19) are used to solve the OPC which can be solved using DP. In order to do so, the states need to be discretized into a finite set. This means that all states at time n has to be on the form $x_n = s_k$ for some integer $k = 1, ..., K$ where the set is denoted $S = \{s_k\}$. The theory stated below is based on the paper *Discrete Time Optimal Control* by T. McKelvey [9] and *Dynamic Programming and Optimal Control* by DP Bertsekas [10].

The solution space will be seen as a directed graph where each node is denoted with the time index, n, and the state value index, k, which means that the number of nodes in the graph will be $N \cdot K$.

We can now define a cost-to-go function, $V_n(s_k)$, to reach a state s_k at time n. The cost-to-go function describes the remaining portion of the additive cost function at some state and at some time [11]. The function is solved recursively and backwards.

$$\begin{aligned} j^*_{n+1,k} &= \arg\min_j f(n, s_j, s_k) + V^*_n(s_j) \\ V^*_{n+1}(s_k) &= f(n, s_{j^*_{n+1,k}}, s_k) + V^*_n(s_{j^*_{n+1,k}}) \end{aligned} \tag{2.22}$$

The star indicates that it is the optimal cost-to-go function $V_n(s_k)$ to reach a new state. The recursion will be initialized with the start state $V^*_1(s_k) = f_{\text{init}}(s_k)$ and the first equation in (2.22) indicate the previous state index which means the state index at time n that leads to the optimal state s_k at time $n+1$. The value iteration will be solved for all $s_k \in S$ which is a finite set of all s_k where $k = 1, ..., K$.

The solution is then to set the initial state as mentioned earlier as $V_1(s_k) = f_{\text{init}}(s_k)$ for $k = 1, .., K$. Then we need to loop this over all times after $n = 1$, i.e. loop over $n = 2, ..., N$, and then solve for all $s_k \in S$. Finally, we will reach time $n = N$ and then we will add the final state cost to get the total cost of the path.

$$V^*(s_k) := V^*_N(s_k) + f_{\text{final}}(s_k) \tag{2.23}$$

The optimal cost will then be for what k^*_N gives the minimal cost $V(s_k)$ where the final state will have the value $s_{k^*_N}$ as

$$\begin{aligned} k^*_N &= \arg\min_k V^*(s_k) \\ V^* &= V^*(s_{k^*_N}) \end{aligned} \tag{2.24}$$

This means that the optimal trajectory x^* will be obtained by a back recursion given by

$$k^*_{n-1} = j^*_{n,k^*_n} \tag{2.25}$$

2.4.2 Lagrangian Relaxation

Constraints are a part of an OPC and when it comes to equality constraints, Lagrangian relaxation is a used method to solve them. Equality constraints can also be solved by introducing new state variables which can cause problem as the dimensions of the state will result in larger computational load. The idea of Lagrangian relaxation is instead to relax the problem by bringing the equality constraint into the objective function with an associated scalar, λ, called Lagrange multiplier. The idea is that if the relaxed problem is solved for a given value of λ, then the solution is also a solution to the original problem [12].

This thesis deals with a constrained shortest path where the directed graph is not only minimized by the cost, but also constrained under an additional constraint which defines how long time the path should take. The equality constraint could be described as

$$\sum_{n=1}^{N-1} f_e(n, x_n, u_n) = t_{\text{end}} \tag{2.26}$$

where t_{end} is the predefined time that the maneuver should take. The cost function would then look like

$$f_L(n, x_n, u_n, \lambda) = f_c(n, x_n, u_n) + \lambda f_e(n, x_n, u_n) \tag{2.27}$$

In order to get the wanted t_{end}, the Lagrangian multiplier will be adjusted so that the cost function is either punished or rewarded until the predefined total time is achieved.

2.5 Simulation Environment

All the simulations for this thesis were done in SPAS, Simulation Platform for Active Safety. SPAS is built on Matlab and Simulink and supports advanced vehicle models with active safety functionality. It also allows for easy setup of customized traffic scenarios.

As the vehicles are in the form of Simulink models, all signals throughout the vehicle can be logged at all times during the scenarios. The vehicles can be controlled autonomously or by a simulated driver.

3

Related Work

This chapter consist of work in different areas related to this project which are used as guidance and inspiration.

3.1 Predictive Cruise Control

There has been previous research in the field of energy optimization. Often, the term predictive cruise control (PCC) is used as future events are taken into consideration. S. Park, H. Rakha, K. Ahn, K. Moran [13] examines the potential of utilizing the topography of the road to better predict an optimal velocity profile. W.H. Lee and J.Y. Li [14] consider vehicle to vehicle and vehicle to roadside unit type of communications. With knowledge of for example future traffic light changes, the number of stops can be minimized. Even though these approaches are interesting and yielded promising results, it assumes additional information about the surroundings rather than focusing only on improving the trajectories of the vehicles.

3.2 Eco Driving

It could be beneficial to look into eco driving, i.e. driving as energy efficient as possible to see what is applicable for autonomous drive. C. Chen et al. [15] test different eco driving approaches of taxi drivers in Beijing and present a list of recommended driving behaviors. The list includes avoiding sharp acceleration, avoiding sharp deceleration, avoid long time acceleration, avoid long time idling and to plan the travel route to avoid road jams.

3.3 Dynamic Programming

There are several work areas where dynamic programming (DP) is well used with good results. Two related studies are presented below where DP is proven to be a

successful method for an adaptive cruise control (ACC) and where the importance of complexity of the models is evaluated.

3.3.1 Using DP for ACC

S. Akhegaonkar, L. Nouvelière, S. Glaser and, F. Holzmann [16] present a longitudinal controller for a smart and green autonomous vehicle (SAGA) in general and an eco ACC in particular. They investigate the impact to use eco ACC on battery electric vehicles (BEV), hybrid electric vehicles (HEV), and plug-in hybrid vehicle (PHEV). They also consider two different environments, city and highway. The optimization is solved by using DP to obtain the optimal acceleration profile and they formulate their objective function as

$$J = Q_1 * Energy + Q_2 * Time \tag{3.1}$$

where they use Q_1 and Q_2 as weight coefficients and J is a function of the acceleration which in return is a function of the torque.

It is shown in the paper that the proposed method using DP to obtain an optimal acceleration profile is successful and can be used for all mentioned vehicle models. However, the control problem has to be modified for HEV:s and PHEV:s since they have two different types of power sources and not one type as for BEV:s. The results vary depending on the environment, speed profiles, and vehicle but the maneuver managed by SAGA is successful and leads to saved energy.

3.3.2 Model Complexity

D. Maarimia, K. Gillet, G. Colin, Y. Chamaillard and C. Nouillant [8] present in their paper the impact of variations of battery parameters on optimal velocity computation of a BEV. The objective is to find the optimal velocity trajectory for a BEV in regard to energy consumption and the optimal control problem (OCP) is solved using DP. The study is done in order to understand the impact of the model's complexity and to find a realistic trade-off between complexity and accuracy of the models. D. Maarimia et al. [8] considered in particular the importance of state of charge (SOC) parameter. The SOC value of the battery influence the current in the battery which as a result has an impact on the power demand of the battery. D. Maarimia et al. saw that by including the SOC of the battery, as an additional state variable, the increased accuracy was negligible. Also, an additional state variable would result in a much higher computational burden which is why that small improvement would not be necessary. D. Maarimia et al. are therefore suggesting simplifying the model regarding the SOC and to assume a constant value through the whole scenario.

4

Methodology

The method is divided into several parts: *4.1 Research Questions* where the questions the thesis aims to answer is presented. *4.2 Setup of BEV* where the creation of the battery electric vehicle in the simulation environment is explained. *4.3 Setup of Benchmark* where aspects and tasks with the traditional ACC is discussed which results in how the benchmark is created. *4.4 Scenarios* where the scenarios are decided and presented. *4.5 Optimal Control Problem Formulation* where the formulation of the Optimal Control Problem is presented. The implementation of the optimization method is described in *4.7 Dynamic Programming Implementation*. Lastly, *4.8 Evaluation* is the subsection where the method for how we will evaluate our implemented ACC function is discussed.

4.1 Research Questions

The thesis can be broken down into two main research questions listed below which this paper aims to answer.

1. What would the energy savings be for the specific traffic situation/s tested?
2. Is it worthwhile to optimize ACC functionality? If so, which aspects of the traditional ACC have the most potential to be optimized?

The energy consumption was measured in a Simulink simulation environment.

4.2 Setup of BEV

To answer the research questions, a battery electric vehicle (BEV) model had to be created which could be run in the simulation environment. The BEV model was created using existing plant models and corresponding controllers from a model library. With the BEV model in Simulink, every signal could be logged and studied. These measurements were then used to model the simplified BEV equations as seen in *2.3 Modelling of a Battery Electric Vehicle*, which is later used in the optimal control problem.

4.3 Setup of Benchmark

With a working BEV model, the performance of a traditional ACC on the BEV had to be evaluated. Our simplified BEV model did not support active safety functionality, however it did include a driver module which converted velocity inputs to pedal actions. To test the energy consumption of a traditional ACC on the BEV, the ACC was tested on a separate more complex vehicle model in the exact same traffic scenario. The resulting velocity and time trajectories of the vehicle were saved. The trajectories could then be fed to the driver of the BEV, which followed the profiles almost exactly. Using this method, the energy consumption of a traditional ACC could be evaluated on a BEV.

Feeding the trajectories to the BEV rather than integrating the ACC functionality, also enables the energy optimized solution to find an optimal trajectory separately from the BEV. Therefore, the energy consumption of the traditional ACC and the energy optimized ACC are measured on the same BEV model using the same type of input, which makes the results comparable.

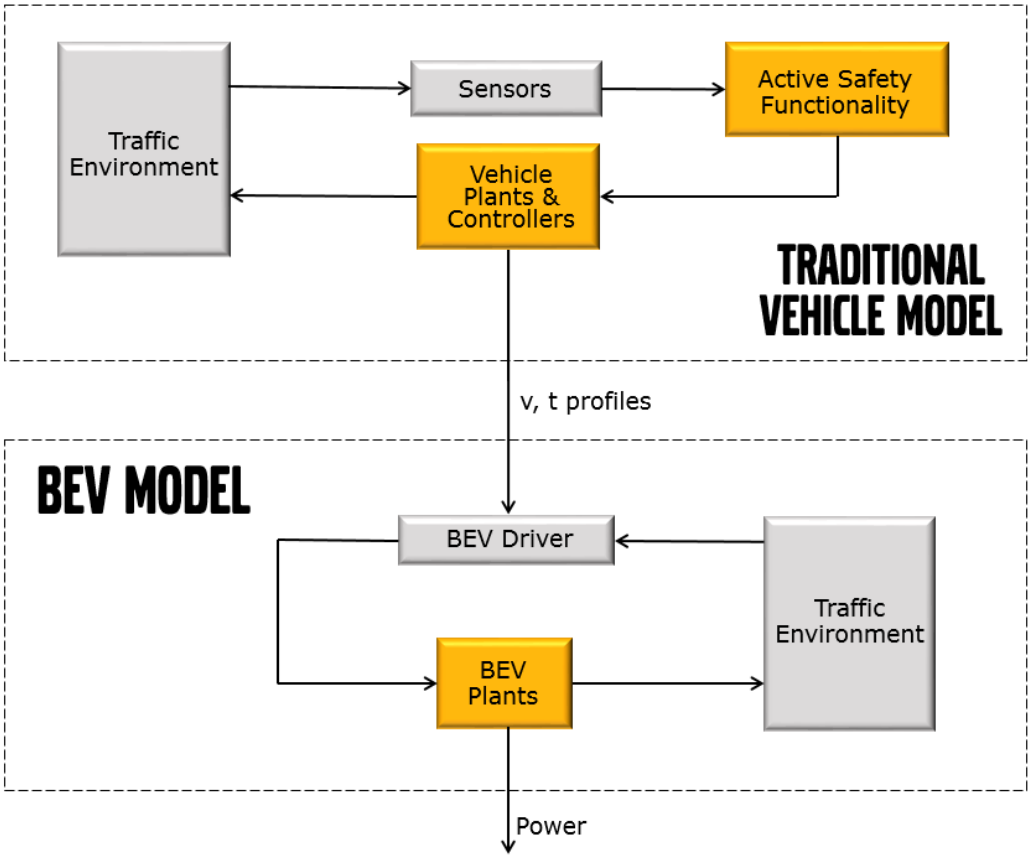

Figure 4.1: Process of running a scenario with the benchmark ACC

The process of estimating the energy from the benchmark ACC is visualized in simplified form in Figure 4.1. The first step was to set up a scenario where the

information about the number of cars, what sort of cars, start and goal speed, and other factors, were defined. This was then run through the traffic environment in the traditional vehicle model which together with the sensors, active safety functionality, and the vehicle plants and controllers forms a closed loop system. When the specific scenario is finished, profiles of the vehicle's velocity at each time step is sent to the BEV model. The profiles are the resulting behavior of the vehicle under control of the ACC. The driver of the BEV follows the trajectory which is sent through the BEV plants in order to obtain the required power. As a result, the total energy usage of the benchmark ACC, E, can be calculated for that specific scenario.

4.4 Scenarios

To identify traffic scenarios with potential to be energy optimized, real life testing of the ACC was done on a new Volvo car by driving around the Gothenburg area. The goal of this testing was to get a better understanding of how the traditional ACC worked, its limitations and find room for improvement. The findings were then discussed with the ACC team at Volvo Cars. Their input was used to decide which traffic situations or aspects of the ACC to focus on. During testing, we identified that deceleration sometimes occur later than necessary. Deceleration is also interesting from a regenerative braking point of view and thus, deceleration scenarios were chosen for further testing.

The scenarios were set up such that they consisted of two vehicles where one was the host vehicle, i.e. the vehicle to be evaluated, and the other one was the target vehicle. The target vehicle was kept at a constant velocity and was driving in front of the host vehicle. The host vehicle had a higher speed compared to the target vehicle. The thesis focus on the deceleration phase as the host vehicle has to adjust its speed in regard to the target vehicle.

For BEV:s, the energy recovery from braking is an important factor which means that friction braking should be avoided. Instead, deceleration should be done through driving resistances such as air resistance, or by regenerative braking which will regenerate energy through the motor. This means that the deceleration profiles had to be evaluated and optimized. More theory on regenerative braking is described in the theory chapter *2.2 Regenerative Braking*.

For this thesis, it was decided to evaluate an energy optimized adpative cruise control (EOACC) for two different relative velocities. One where the host vehicle had a start velocity of 100 kph and the target vehicle had a constant velocity of 40 kph. This is referred as the $100 - 40$ case. The second case was when the host vehicle had a speed of 60 kph and the target vehicle had the same as speed as in the first scenario, 40 kph. This case is referred to as the $60 - 40$ case.

From the benchmark, two different velocity curves where then obtained by driving those two velocity scenarios, $100 - 40$ and $60 - 40$. Both simulations where run for

a longer time than the actual deceleration took. That enabled us to create four (4) different scenarios for each velocity scenario, i.e. 8 different scenarios in total were created.

The first scenario, referred as (1), is based on the deceleration phase of the benchmark, i.e. the traditional ACC. It was achieved by using a very large initial relative distance to see when the benchmark vehicle started to adapt to the vehicle in front. The distance at which the benchmark started to adapt was then used as the initial relative distance for the EOACC. The same total maneuver time and final relative distance were also used.

The second scenario, (2), includes the deceleration phase of the first scenario, plus an additional 10 seconds before the benchmark vehicle began to decelerate. This is implemented by letting the EOACC see the target vehicle at a larger distance as well as adding 10 additional seconds to perform the maneuver. The larger distance is calculated as the equivalent of 10 seconds of constant velocity at the initial velocity of the host vehicle. This allows the EOACC to test the potential energy improvement of decelerating earlier.

Similarly to the second scenario, the third scenario, (3), was created by giving the vehicle 10 additional seconds to reach the goal state. In this case the initial and final relative distances are unchanged and only the total time is adjusted.

Finally, for the fourth scenario, (4), 10 seconds were added both to the beginning and to the end of the original deceleration phase as to test the combined effect of reacting earlier and longer. The initial relative distance is increased in the same way as for scenario (2).

All velocity profiles of the benchmark were compared to the EOACC. The different scenarios tested in this thesis are presented in the table below.

List of Scenarios			
Scenario	Velocity Profile [kph] (v_1, v_N)	Distance Profile [m] (d_1, d_N)	Time [sec] t_{end}
100 - 40 (1)	100 - 40	127 - 17	17
100 - 40 (2)	100 - 40	297 - 17	27
100 - 40 (3)	100 - 40	127 - 17	27
100 - 40 (4)	100 - 40	297 - 17	37
60 - 40 (1)	60 - 40	90 - 18	34
60 - 40 (2)	60 - 40	144 - 18	44
60 - 40 (3)	60 - 40	90 - 18	44
60 - 40 (4)	60 - 40	144 - 18	54

Table 4.1: Scenario parameters

The left most column presents the scenario's number and whether it is a 100-40 or a 60-40 scenario. The second column lists the velocity of the first and final state v_1,

v_N. The third column lists the relative distance between the vehicles of the first and final state d_1, d_N. The total time of each scenario, t_{end}, is listed in the final column. The end time which is an equality constraint is fulfilled by the EOACC through the use of Lagrangian multipliers, explained in the theory section *2.4.2 Lagrangian Relaxation*.

As the first and final state will be the same for both the benchmark and the EOACC, the results will be comparable, and any improvements will be the effect of a better velocity profile. Note that the time is fixed in all scenarios, this is equivalent to a fixed driven distance compared to the ground. The results from the scenarios are presented in table 5.3 in result section *5.2 Results from Scenarios*.

The second thing we wanted to look into was the trade-off between the energy consumption and the time taken to fulfill the end state. The trade-off were visualized as a Pareto Front which can be seen in the result section *5.3.1 Pareto Fronts*. For each Pareto Front, a predefined end time, t_{end}, was defined. In order to make the results comparable, an extra state of constant velocity had to be added to make all the scenarios have the same end time. This means that for scenarios where the time taken to reach the end was short, the vehicle had to stay at the end velocity until the predefined end time was reached. Therefore, reaching the end state quick does not necessarily result in the smallest amount of energy usage.

4.5 Optimal Control Problem Formulation

After creating the benchmark standard, the procedure for data collection, and the scenarios, the development of an EOACC was started. The first step was to formulate the optimal control problem (OCP).

Since the thesis aimed to optimize the energy consumption of a BEV for specific scenarios, it is obvious that one solution would be to stop completely unless the problem is constrained. The problem had to be constrained such that the desired goal state would be reached within a reasonable amount of time. A single objective OCP was formulated where the time was taken as an hard equality constraint to be able to make direct comparisons with the benchmark. The time each scenario should take is denoted as t_{end} and an initial and final velocity v_{init} and v_{end}, were predefined for each scenario, see table 4.1. The same is true for the relative distance d which also has a predefined initial and final value. It is important for safety reasons that the relative distance never is lower than the predefined final relative distance. The objective function is to minimize the energy, where J in equation (4.1) is the integral of the power. The power can be either positive or negative depending on whether energy is consumed or regenerated. Based on the energy cost function and the constraints, the minimization problem was formulated as below, equation (4.1).

$$
\begin{aligned}
\min J = \int_0^{t_{\text{end}}} & P_{\text{batt}}\Big(v(t), a(t)\Big)dt \\
\text{s.t. } & v_{\min} \leq v(t) \leq v_{\max} \\
& a_{\min} \leq a(t) \leq a_{\max} \\
& d_{\text{end}} \leq d(t) \\
& v(0) = v_{\text{init}} \\
& v(t_{\text{end}}) = v_{\text{end}} \\
& d(0) = d_{\text{init}} \\
& d(t_{\text{end}}) = d_{\text{end}} \\
& t \in [0, t_{\text{end}}]
\end{aligned}
\tag{4.1}
$$

The relationship between the power, P_{batt}, and the velocity and acceleration are described in the theory section 2.3 *System Description*. In particular by the equations 2.3.1-2.16 within that section.

By further using the theory stated in section 2.4 *Dynamic Programming*, the OCP could be discretized and solved using and dynamic programming.

4.6 Optimization Method

There are multiple ways to solve an OCP and a few options were considered, mainly dynamic programming (DP) and model predictive control (MPC). DP is discussed in more detail in the theory section 2.4 *Dynamic Programming*.

MPC works by solving the OCP only a certain period into the future, and using only the first part of the solution as the control signal. The process is repeated for the updated states. Continuously updating the optimal control sequence has some obvious advantages. Especially as the traffic situation changes, e.g. the target vehicle may turn or accelerate, it is necessary for a real ACC to adapt to these changes.

There are also some disadvantages, mainly that the OCP has to be solved for every iteration of the MPC. This is very computationally heavy and for the purpose of this thesis, not fully necessary. The aim of this thesis is not to develop a new ACC but rather to show the potential of optimizing the ACC. Using simulation, the traffic situation could be constrained such that the behavior of the target vehicle is known. The OCP could then be solved once with no need to update the solution, making the use of MPC unnecessary [17].

DP was chosen as it can be used to generate a complete optimal control sequence for the whole scenario, given that the target behavior is known. As this can happen offline, no integration with the BEV model in the simulation environment has to be

done while the simulation is running. The optimal trajectory can simply be used as an input to the BEV driver. The problem at hand is also highly non-linear which makes the approach of the DP to break down the problem into subproblems a good strategy. Furthermore, DP been proven successful for other similar projects [8], [16].

4.7 Dynamic Programming Implementation

The minimization problem stated above was solved by Dynamic Programming (DP) which is a method to solve OCP:s. The method determined the velocity trajectory that minimized the energy usage subject to the constraints. The velocity and time profiles were obtained, which later were used as input for the BEV model to measure the actual energy consumption.

We used the theory stated in equation (2.21) to formulate the OCP in a standard way.

$$x^* = \arg\min_x \left\{ f_{\text{init}}(x_1) + f_{\text{final}}(x_N) + \sum_{n=1}^{N-1} f(n, x_n, x_{n+1}) \right\} \tag{4.2}$$

As mentioned before, the cost function was based on the theory described in theory section *2.3 Modelling of a Battery Electric Vehicle*. The scenarios only consisted of longitudinal movement, and only forces in that direction were included. Two state variables were used to describe the host vehicle's movement as

$$x_n = \begin{bmatrix} v_n \\ d_n \end{bmatrix} \tag{4.3}$$

where v_n and d_n are the velocity of the host vehicle and the relative distance between the host and target vehicles at time n, where $n = 1, ..., N$. I.e., $n = 1$ described the initial state and $n = N$ described the final state.

The initial and final cost functions, i.e. the cost to reach the first and final state, f_{init} and f_{final} seen in equation (4.2) had to be defined. As each scenario had specific initial and final state, all other starting and final states had to be eliminated or made infeasible for the optimal solution. This was achieved by the equations below, which would force the optimal solution to consist of the predefined initial and final state.

$$f_{\text{init}}(x_n) = \begin{cases} 0, & x_n = x_1 \\ \infty, & x_n \neq x_1 \end{cases} \tag{4.4}$$

$$f_{\text{final}}(x_n) = \begin{cases} 0, & x_n = x_N \\ \infty, & x_n \neq x_N \end{cases} \tag{4.5}$$

Essentially, if x_n was not equal to x_1, then an infinite cost would be added, which would not be included in an optimal solution of the OCP. This means that no initial states other than x_1 would be chosen. Similarly, the final state would not be chosen to anything else than x_N.

In addition, the general cost function for all other state transitions had to be defined. From equation (2.20) in theory section *2.4 Dynamic Programming*, the cost function for all other state transitions could together with f_{init}, f_{final}, be written into a single function f as

$$f(n, x_n, x_{n+1}) = \begin{cases} f_{\text{cost}}(1, x_1, q_u(1, x_1, x_2)) + f_{\text{init}}(x_1), & (x_1, x_2) \in \mathcal{X}_1 \\ f_{\text{cost}}(n, x_n, q_u(n, x_n, x_{n+1})), & (x_n, x_{n+1}) \in \mathcal{X}_n \\ f_{\text{cost}}(N-1, x_{N-1}, q_u(N-1, x_{N-1}, x_N)), & (x_{N-1}, x_N) \in \mathcal{X}_{N-1} \\ \infty, & (x_n, x_{n+1}) \notin \mathcal{X}_n \end{cases} \tag{4.6}$$

where q_u described the control variable u_n, and $\mathcal{X}_n$ describes the set of feasible state transitions. The construction of how the energy is calculated from the state changes is shown in steps in section *2.3 Modelling of a Battery Electric Vehicle* through section *2.3.4 Battery Model*. The OCP could then be reformulated as

$$x^* = \arg\min_x \left\{ \sum_{n=1}^{N} f(n, x_n, x_{n+1}) \right\} \tag{4.7}$$

The states and transitions can be visualized as a directed graph. Figure 4.2 shows the states and the cost of every state transition.

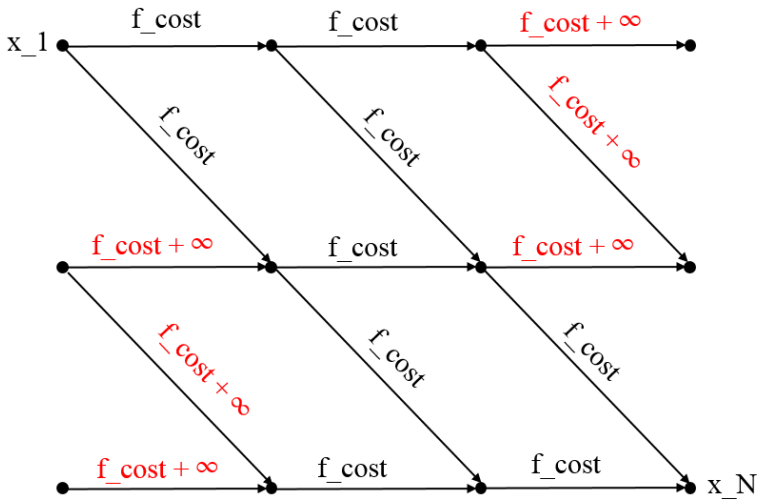

Figure 4.2: State transitions in directed graph

In Figure 4.2, it is illustrated how the initial and final cost functions force the graph to take a specific path. In the upper left corner of the Figure, is the desired initial state x_1. Since the graph is of dimension $N \cdot K$, the possibility to start in another state had to be removed. By using the definitions stated in equation (4.4) and (4.5), infinity costs were added to the transitions from other initial states than x_1, see the red marked costs. In the same way, going to other states than x_N at time N would result in an infinite cost, which will remove that option from the optimal solution. Further methodology about the directed graph is described in section *4.7.1 Directed Graph Design*.

As stated in theory section *2.4.2 Lagrange Relaxation*, it is possible to relax the problem by taking an equality constraint and put it into the objective function. To make the results of the EOACC and the benchmark comparable, the total time of a scenario is fixed, i.e. an equality constraint. Lagrangian Relaxation was therefore used to constrain the time. This was done by formulating the new cost function, f_{relaxed} as

$$f_{\text{relaxed}} = f(n, x_n, x_{n+1}) + \lambda f_{\text{time}}(n, x_n, x_{n+1}) \tag{4.8}$$

where f is the cost function expressed in equation (4.6) and f_{time} describes the time taken to go from state x_n to x_{n+1} at index n. The final OCP could then be expressed as

$$x^* = \arg\min_x \left\{ \sum_{n=1}^{N} f(n, x_n, x_{n+1}) + \lambda f_{\text{time}}(n, x_n, x_{n+1}) \right\} \tag{4.9}$$

where λ is the Lagrangian multiplier that was manually adjusted. To reach the final state in a shorter time, the Lagrangian multiplier should be increased and to achieve a longer time, it should be decreased.

4.7.1 Directed Graph Design

The design of the directed graph is based on the theory in section *2.4 Dynamic Programming*. x_n was used to represent the state at index n where $n = 1, ..., N$. For each index n there were K possible states, s_k, where $k = 1, ..., K$. The states at each index n were a finite set of possible velocities of the host vehicle.

The index was contrary to the example given in the theory subsection *2.4.1 Bellman-Ford Algorithm*, not defined as time but rather as the relative distance between the host and the target vehicle. As the scenarios studied only looks at deceleration, the host velocity was for every state except the goal state higher than the target velocity. Thus, for the increasing index n, the relative distance was always decreasing. For the final n, the desired relative distance and the target velocity was reached. The number of nodes, i.e. possible states in the graph were $N \cdot K$.

There is no specific reason for using the relative distance instead of time as one of the states. It was chosen as it was more natural to work with for the specified scenarios. The results are the same in both cases.

The cost function f, which calculates the energy required to transition from one state to the next was modelled according to section *2.3 Modelling of a Battery Electric Vehicle*. A graph could therefore be created with the costs as edge weights. It had already been determined that the relative distance was always decreasing. Therefore, the graph was directed such that the index n was strictly increasing for every state transition. An example of how the directed graph could look is presented below in Figure 4.3. Note that the actual directed graph has a lot more states and possible transitions than shown in the Figure.

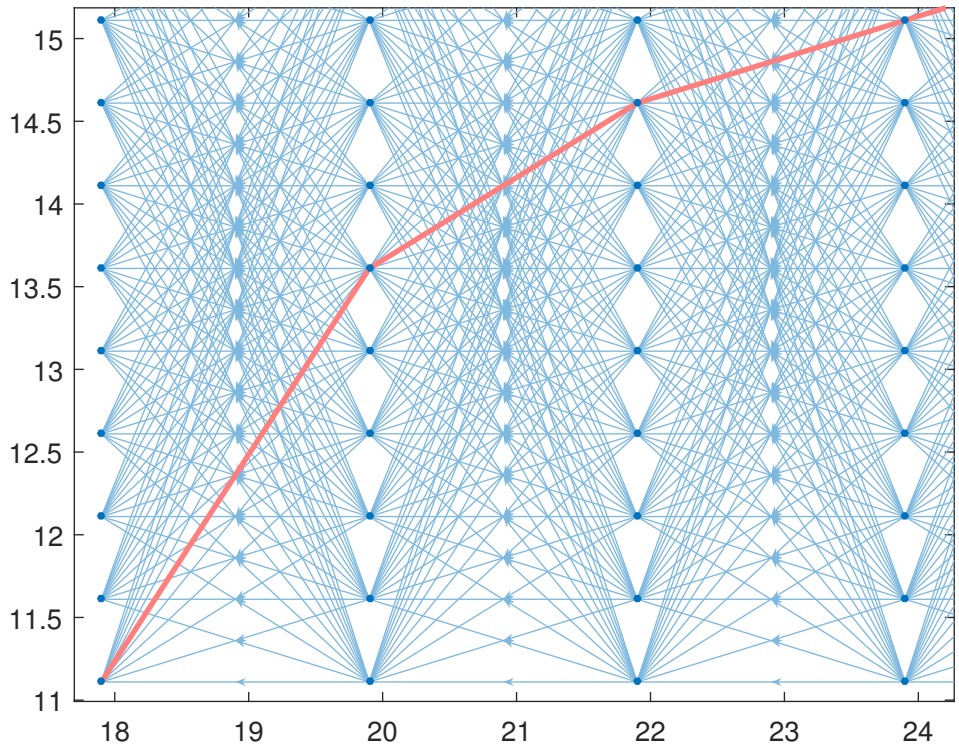

Figure 4.3: Zoomed in view of a directed graph with a reduced number of states

As one can see in Figure 4.3, each node is connected by several lines which represents the transition steps. On the x- and y-axis, the state's distance gap and velocity are presented respectively. The node to the bottom left is the goal node, $n = N$. For every state change, n increases by one which is equivalent to moving one column to the left in the directed graph. For each step, the velocity of the host vehicle can increase, be constant, or decrease any number of steps within the directed graph.

The constraints were implemented as infinite edge costs as it was more computationally effective than to only connect the feasible connections when constructing

the graph. That includes state changes which resulted in very large accelerations, both positive and negative. The code which generated the graph also had to be constructed in such a way that it could either allow or disallow increasing the velocity.

For this thesis, we decided on the following constraints for the graph.

1. Maximum acceleration and deceleration of -3.5 and 2 m/s^2 respectively [5]
2. State transitions with infinity time maneuver had an infinite cost

4.8 Evaluation

We did not have the same ability to study individual signals in a real car compared to in a simulation environment. Hence some verification was necessary to confirm that the behavior found from simulations is comparable to how the real car behaves in traffic and vice versa.

4.8.1 Cost Function

The cost function is modelled after the BEV model in Simulink and calculates the energy required for state changes of the directed graph. The cost function follows the theory in section *2.3 Modelling of a Battery Electric Vehicle*. It is important to verify this model against the actual BEV model.

The cost function assumes linear velocity changes between states, thus the time steps between states become relevant. Too large steps might lead to inaccurate results. The cost function will therefore be evaluated using different time steps to make sure they will not significantly influence the results.

To verify the model, a velocity profile with a very large number of data points will be used as a benchmark. The velocity profile will be tested on the BEV, and the motor power as well as other parameters such as torque and mechanical efficiency will be measured. The same velocity profile will then be used with the cost function but with a reduced number of data points and the same parameters will be measured. Reducing the number of data points represents increasing the time step between them and a few different step sizes will be tested, from 1 second down to 0.05 seconds.

4.8.2 Results

When obtaining the optimized trajectories, it was necessary to ensure that all constraints were fulfilled. This was done by logging all parameters that were affected

by a constraint, e.g. the distance gap between the vehicles. The results were also evaluated regarding their feasibility.

At the time of writing, there were no BEV available on the market from Volvo Cars. Therefore, we did not have the possibility to verify the BEV model against reality. To further understand if the BEV model and the EOACC solution were feasible, close discussions with people at Volvo Cars were held. Therefore, while the BEV model may not be a perfect estimation of reality, it should be reasonably accurate. To make the results of the EOACC and the benchmark comparable we made sure to run the tests on the same BEV model.

5

Results

This chapter presents all relevant results. The first section, *5.1 Cost Function*, shows the results from verifying the cost function with the BEV model in SPAS. This to ensure that the cost function, based on equations stated in the theory chapter, was giving reasonable values compared to the BEV model.

The second section *5.2 Results from Scenarios* presents the energy savings from the chosen scenarios and is followed by the sections *5.2.1 Scenarios 100-40 kph* and *5.2.2 Scenarios 60-40 kph* in which each scenario is analyzed in more detail. These sections include both velocity and energy plots which are all compared to the benchmark.

The third section *5.3 Energy versus Time Trade-off* compares a time optimal and an energy optimal solution. The trade-off is presented as Pareto fronts for both the $100-40$ and $60-40$ case. It also shows the benchmark in relation to the Pareto fronts.

5.1 Cost Function

To apply the methods discussed in *4 Methodology*, an accurate cost function was developed. The cost function uses two states as input and outputs the energy cost for transitioning between the states. The cost function is based on the theory in *2.3.1 Motion Equations*, *2.3.2 Transmission Model*, *2.3.3 Electric Machine Model* and *2.3.4 Battery Model*.

To verify the cost function, different test scenarios were run on the BEV model. The velocity profile and the power required by the electric motors were measured. Spaced out data points from the velocity profiles were then used as inputs for the cost function. Different spacings, or time steps were tested and the results were compared to the power measured directly on the BEV model.

The cost function is limited in that it assumes linear velocity change between two states. It is therefore important to know how small the time steps have to be in order to achieve an accurate result. Especially since the optimization problem will take a long time to solve for very fine steps.

Looking at the following two scenarios, the accuracy of the cost function can be determined. The first scenario is a fast deceleration scenario from $100-40$ kph in 19 seconds. The second is a slower deceleration from $60-40$ kph in 60 seconds. The scenarios were chosen as they are very different in both time and velocity profile.

Starting with the $100-40$ kph scenario, the power required by one motor calculated by our cost function, compared to the actual values from the BEV model can be seen in Figure 5.1. The sub-figures show the power plots for different time steps. The tested time steps, i.e. time between states range from 1.0 seconds down to 0.05 seconds.

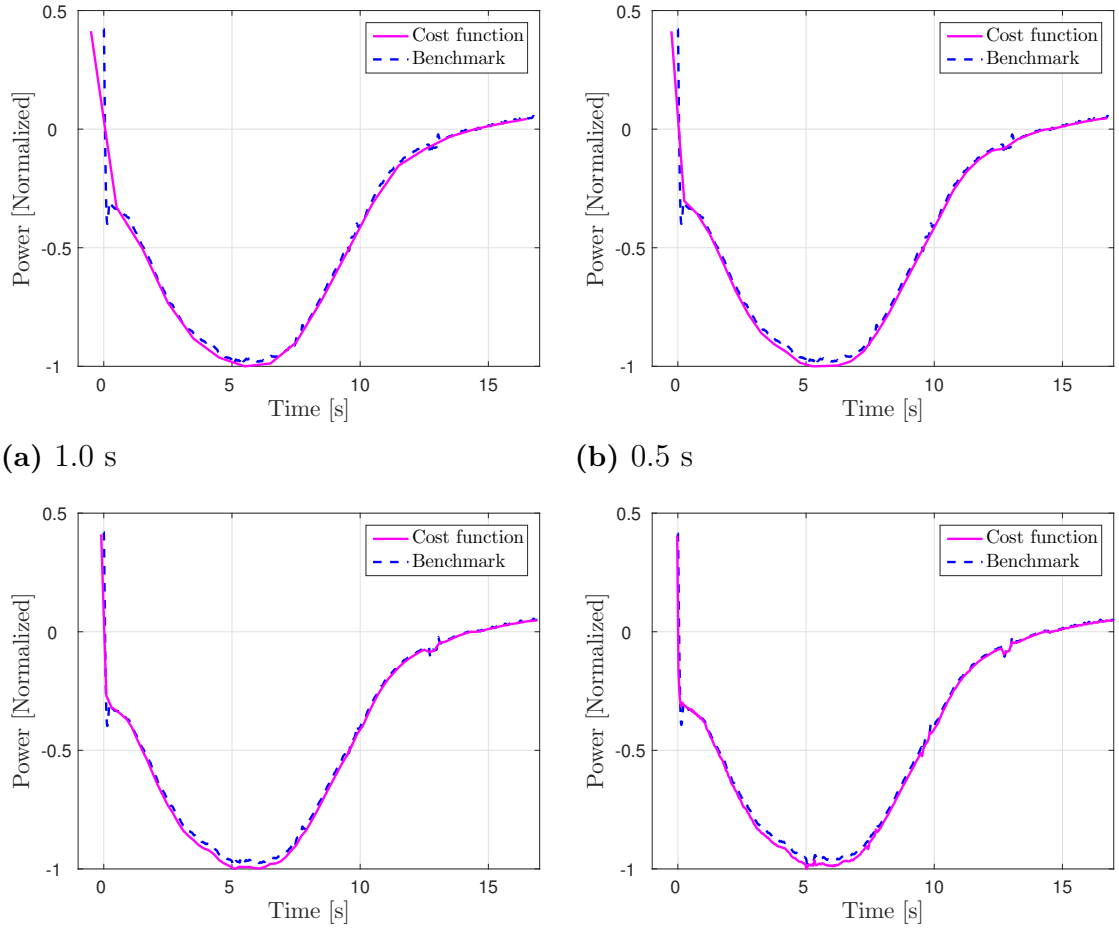

(a) 1.0 s **(b)** 0.5 s

(c) 0.2 s **(d)** 0.05 s

Figure 5.1: Power required for a 100-40 kph case with different time steps

Unsurprisingly, smaller time steps yield more accurate results. The exact values of the error can be seen in table 5.1. The energy is the integral of the power curve. Since the values are discrete, the integral is calculated as the power multiplied by the corresponding time step. Note that the power is calculated between states, not at states.

Most importantly is that the accuracy does not greatly increase with smaller steps

and any error beyond 0.05 s is most likely due to other causes. By decreasing the step size from 0.2 s to 0.05 s, the total energy error remains at -3.12 %.

Step size is most important when the acceleration, and thus also the power, change rapidly. In sub-figure 5.1a, at the beginning of the scenario, the power makes a large change rapidly. With step size of 1 second, the difference is clearly visible. Using larger step sizes would reduce the solution space as solutions with quick changes would not be found in the directed graph. For the remaining sub-figures the error of the rapid change becomes smaller as the step size decreases.

Large quick changes in acceleration are also expected from the solution generated by the directed graph due to how it is constructed, see section *4.7.1 Directed graph design*.

Cost function comparison with different time steps	
Time step [s]	Total energy error [%]
1	-3.15
0.5	-3.13
0.2	-3.12
0.05	-3.12

Table 5.1: Estimated energy error of the cost function compared to the BEV with different time steps for the $100 - 40$ kph case

Looking at the other scenario, i.e. $60 - 40$ kph in 60 seconds, the results are similar. The required power of one motor for the $60 - 40$ kph scenario is plotted in Figure 5.2 where again, each sub-figure represents a different time step. Again, the accuracy increases for smaller time steps but only very slightly and it is most evident for fast changes in power. The exact results can be seen in table 5.2.

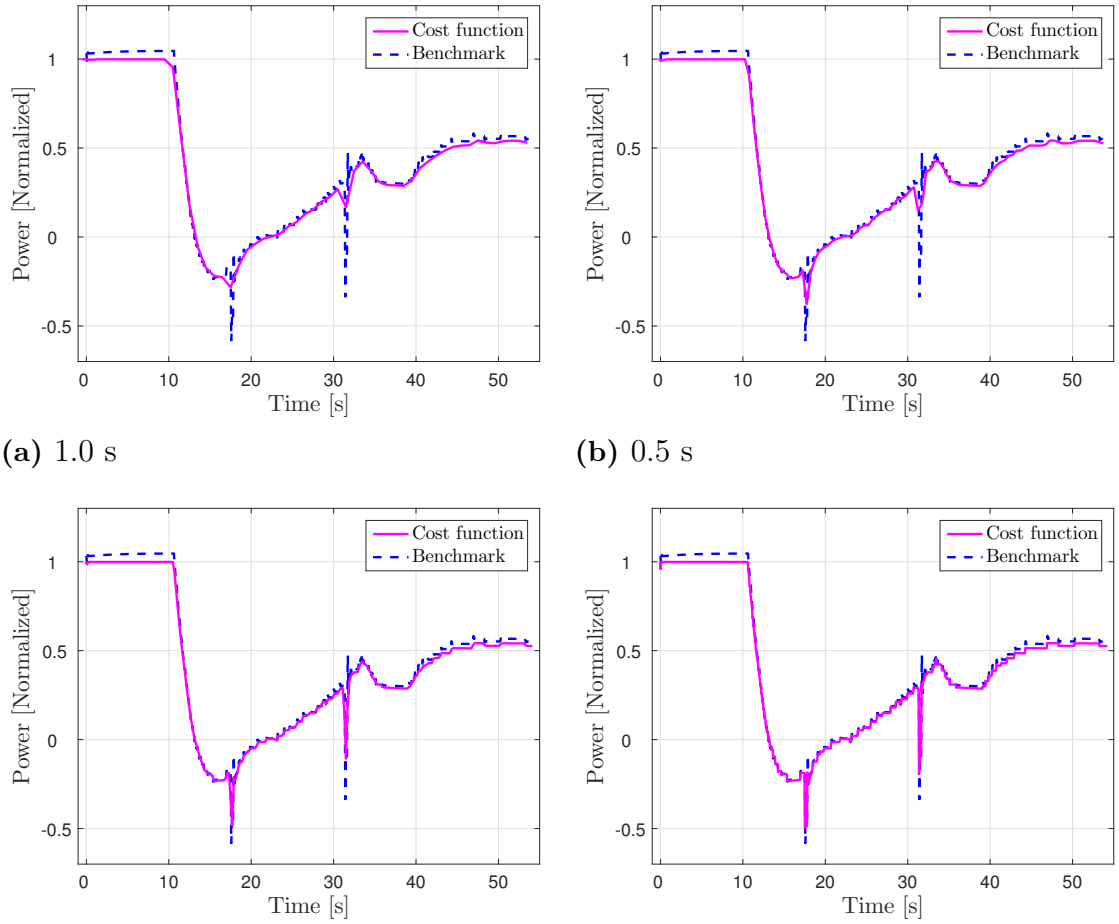

(a) 1.0 s

(b) 0.5 s

(c) 0.2 s

(d) 0.05 s

Figure 5.2: Power required for a 60-40 kph case with different time steps

Cost function comparison with different time steps	
Time step [s]	Total energy error [%]
1	-4.76
0.5	-4.75
0.2	-4.73
0.05	-4.72

Table 5.2: Estimated energy error of the cost function compared to the BEV with different time steps for the $60 - 40$ kph case

While the energy error is almost 5 %, it is very consistent and always lower than the values measured on the BEV. When comparing with the $100 - 40$ kph scenario in table 5.1, the largest difference in error is about 1.5 %. Thus, the conclusion from this section is that the cost function consistently estimates the energy a bit lower than the actual value. However, with such consistent results, the desired behavior

of the vehicle should be very similar using either the cost function or the actual BEV model. Regarding the time steps, a smaller time step is of course better but anything less than 1 second should yield decent results. Anything below 0.5 seconds is definitely good enough for our purpose as we do not require an accuracy of one per thousand and we have larger inaccuracies elsewhere.

The time steps for the actual scenarios will vary. This is due to the design of the directed graph. The plots below show the size of the time steps for scenario (1), $100 - 40$ kph.

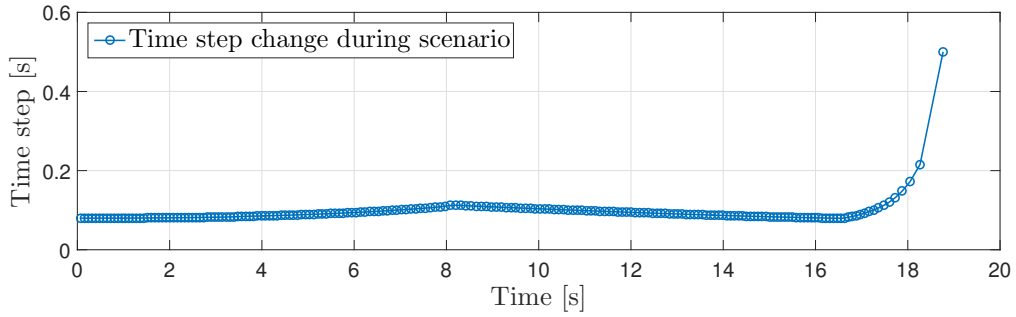

(a) Time steps size during scenario

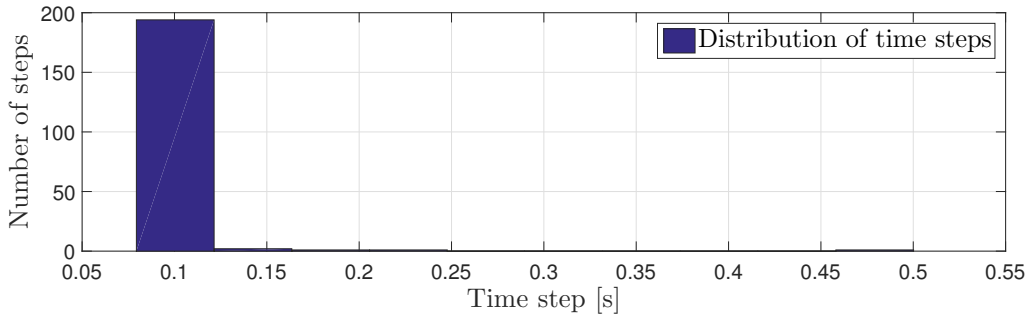

(b) Distribution of time step sizes

Figure 5.3: Distribution of time step sizes during a $100 - 40$ kph scenario

Figure 5.3a shows how the size of the time steps vary throughout the scenario. When construction the directed graph, we define the relative distance steps and not the time steps. If all the relative distance steps were equal, the corresponding time would increase as the relative velocity becomes lower. At very low relative velocity the time steps become much longer as it takes a long time to cover a short relative distance. To combat the longer and longer time steps, the relative distance steps are logarithmically spaced where the shortest steps are close to the target velocity.

Figure 5.3b shows the distribution of different time step sizes. Almost all of the time steps are below 0.2 seconds. This behavior is similar throughout all the scenarios where only the last or the last few steps are above 0.5 seconds.

5.2 Results from Scenarios

List of scenarios and their respective energy savings				
Scenario	Velocity profile [kph]	Start distance gap [m]	Time [s]	Energy savings [%]
100 - 40 (1)	100 - 40	131	19	2.10
100 - 40 (2)	100 - 40	300	29	39.10
100 - 40 (3)	100 - 40	131	29	5.46
100 - 40 (4)	100 - 40	300	39	70.85
60 - 40 (1)	60 - 40	87	40	1.98
60 - 40 (2)	60 - 40	140	50	5.00
60 - 40 (3)	60 - 40	87	50	0.77
60 - 40 (4)	60 - 40	140	60	4.43

Table 5.3: Energy savings for all scenarios

In table 5.3 you will find all the predefined scenario settings such as distance, time, and velocity profile. All scenarios are defined according to the methodology section *4.4 Scenarios*. The first column in table 5.3 labeled *Scenario*, describes which scenario each row is representing. The column labeled *Velocity profile* describes the velocity the host vehicle is initially starting with, which is the first number, and the target vehicle's velocity, which is the second number. In other words it describes the host vehicle's velocity at its start and end states. In the column labeled *Start distance gap*, the initial distance between the host and target vehicle is presented. Similarly the time for the vehicle to reach the defined goal state is presented in the column labeled *Time*. Lastly, the column labeled *Energy savings* is the energy usage for the benchmark compared to the energy usage for the EOACC.

For each scenario (1)-(4), different maneuver times and start distances are used. The four different scenarios can shortly be described as

- **Scenario (1):** The actual start distance and maneuver time it takes for the benchmark vehicle
- **Scenario (2):** Scenario (1) with added 10 seconds in the beginning
- **Scenario (3):** Scenario (1) with added 10 seconds in the ending
- **Scenario (4):** Scenario (1) with added 10 seconds in the beginning and ending

A more thorough explanation can be found in section *4.4 Scenarios*. The results from each velocity profile $100 - 40$ kph and $60 - 40$ kph, and its respective four different scenarios are analyzed in more detail in the following sub-sections.

5.2.1 Scenarios 100-40 kph

In this section, all four scenarios, see row $1-4$ in table 5.3, are presented. Which means that the host vehicle is always having $[100, 40]$ as its start and end velocity state, while the distance gap and maneuver time is different for each scenario.

This section includes the plots of the host's velocity profile, and how the profile affects the energy usage during the scenario. The results are compared to the benchmark's results which are also included in the plots.

Below are four plots, one for each scenario. The green line represents the EOACC vehicle, while the red dashed line is the benchmark. Note that the initial and final states are identical for both the EOACC and the benchmark. Therefore, since the target vehicle has a constant velocity, the average velocity of the host vehicle must be the same for both the EOACC and the benchmark.

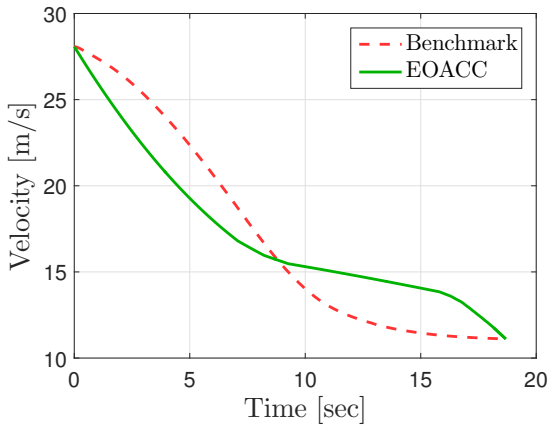

(a) Scenario 100-40 kph (1)

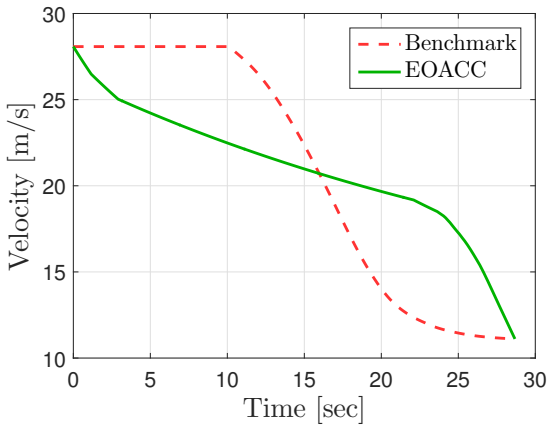

(b) Scenario 100-40 kph (2)

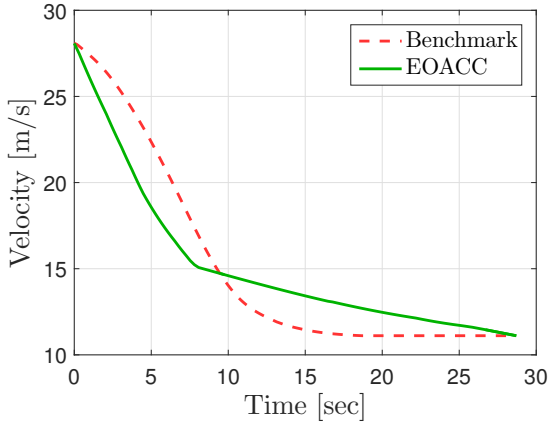

(c) Scenario 100-40 kph (3)

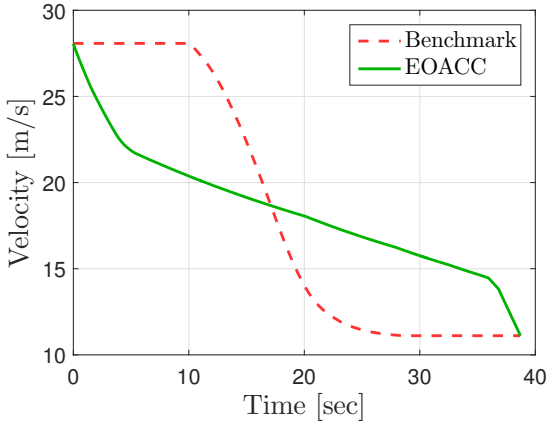

(d) Scenario 100-40 kph (4)

Figure 5.4: Velocity plots for all tested $100-40$ kph scenarios

Scenario (1) is presented in sub-figure 5.4a which shows the velocity profile for the time it takes for a vehicle with the benchmark ACC to decelerate from 100 to 40

kph. The host vehicle starts to adapt to the vehicle in front at a distance gap of 131 meters and the maneuver takes 19 seconds.

The EOACC vehicle chose a relative lower speed after the initial state compared to the benchmark vehicle. In general, a lower velocity is beneficial in regard to energy consumption. The average velocity over the whole scenario has to be equal in both cases. This is because the total scenario time and the initial and final relative distances are the same for the EOACC and the benchmark, and the target vehicle has a constant velocity. Therefore, the EOACC has to have a higher velocity later in the scenario to compensate for the lower velocity in the beginning. The switch happens after approximately 9 seconds. The behavior is most clearly visible in sub-figure 5.4d.

The reason for this specific behavior is that the energy losses are exponential in regard to velocity. Hence it is more advantageous to have a lower speed compared to the benchmark in the beginning despite having a higher speed near the end. This behavior is influencing all scenarios and is most obvious in scenarios where the benchmark does not immediately brake.

Scenario (1) results in an improvement of 2.10% compared to the benchmark which is listed in table 5.3. The percentage is very small compared to the remaining scenarios for $100 - 40$ kph. The reason for this is because of the small room for improvement. Since the scenario is defined under strict constraints such as a large velocity change during a short time window, the solution space is limited and there is not much opportunity to coast.

Next scenario, (2), is when the EOACC vehicle is allowed to adapt to the target vehicle 10 seconds before the benchmark does. This is clearly visible in sub-figure 5.4b. The benchmark has a constant speed of 100 kph the first 10 seconds while the EOACC vehicle is adapting from $t > 0$.

The total maneuver time for scenario (2) is 29 seconds since the original deceleration phase took 19 seconds. The EOACC vehicle decelerates slower than the benchmark until $t \approx 24$ before braking by approximately the same gradient as the benchmark. Reacting 10 seconds earlier results in an improvement of 39.10%.

Scenario (3) is the case when 10 seconds are added to the end of the original maneuver, the total time is 29 seconds. This means that the initial distance gap between the vehicles were the same as for scenario (1), i.e. 131 meters. But the driven distance is greater since the maneuver time is longer. 10 extra seconds with the same initial conditions resulted in an improvement of 5.46%.

Scenario (4) is a combination of scenario (2) and (3) which means that a time of 10 seconds is added both before and after the actual deceleration phase of the benchmark. The total time for scenario (4) is therefore 39 seconds. This enables the EOACC vehicle to adapt in advance, and also allows for a longer maneuver time. The velocities from the benchmark and the EOACC are plotted in sub-figure 5.4d.

The velocity curve of the benchmark for scenario (4) is as expected. It is the same as

scenario (1) but with 10 seconds of constant velocity added to the beginning and to the end of the maneuver from scenario (1). The EOACC curve is adapting from the beginning until the end of the total scenario time. The EOACC vehicle decelerate less during a longer time which means that it does not require power from the motor to keep up with the target vehicle in front.

Scenario (4) resulted in an improvement of 70.85% which is the greatest percentage value of all the four cases. This is expected since the room for improvement is the largest. The absolute energy savings for scenario (4) is about 5.6 % larger than for scenario (2) and (3) combined.

To see where energy is saved during the scenario and whether any specific behaviors can be identified as energy efficient or inefficient the power plots are studied. The power in all four cases are plotted below in Figure 5.5.

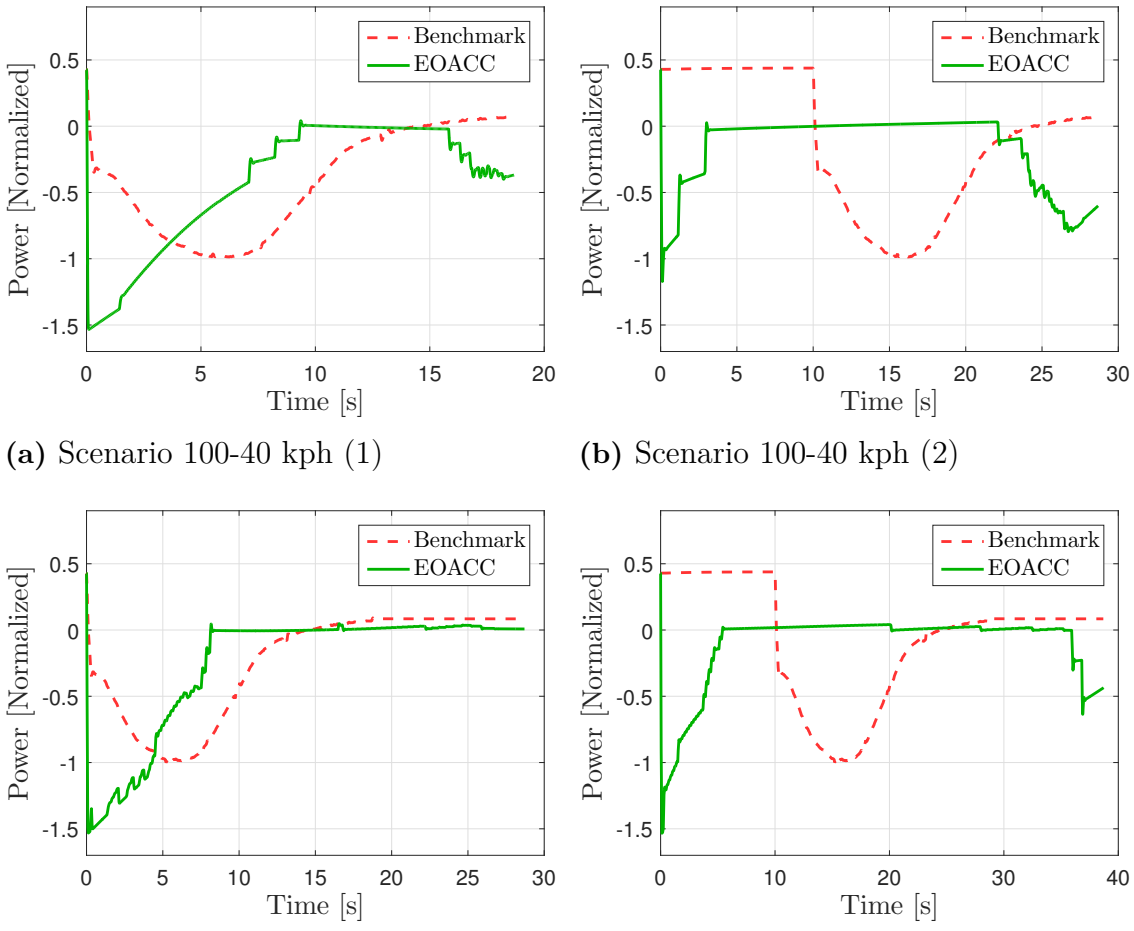

(a) Scenario 100-40 kph (1)

(b) Scenario 100-40 kph (2)

(c) Scenario 100-40 kph (3)

(d) Scenario 100-40 kph (4)

Figure 5.5: Energy plots for all tested $100-40$ kph scenarios

The power for every $100-40$ scenario can be seen in Figure 5.5. Notably, the power curve of the EOACC in all four scenarios jumps between different values. This is because the power is heavily dependent on the acceleration and that the acceleration

profile is originally discontinuous due to the construction of the directed graph. However, the plotted results are the output from the BEV model, which shows that it was able to follow large jumps in acceleration.

For all scenarios, it is evident that most of the energy saved is from the deceleration during the first part of the scenarios. However, once the benchmark start to decelerate faster than the EOACC, the benchmark regenerates more energy.

In scenario (1), (2) and (4), the EOACC decelerates near the end to reach the goal velocity at the specified end time. The final deceleration is also visible in the energy plots.

Most interestingly is that the EOACC for all scenarios has periods where the power is kept around zero Watt. This behavior is known as coasting. The vehicle simply decelerates through drag and rolling resistances. Coasting is the most energy efficient way of preserving energy since regenerating energy has losses in addition to drag and rolling resistances. There are also additional losses once the energy has to be used again to maintain speed. Coasting is therefore preferred if possible.

For scenario (1), (2), (3), and (4) the savings were 2.10 %, 39.10 %, 5.46 %, and 70.85 % respectively as seen in table 5.3. If the consumed and regenerated energy is similar in size, the total energy will be close to zero. The energy improvement percentage will therefore be more significant compared to a case where the total energy is far from zero, even though the same amount of energy is saved. Thus, measuring energy improvement in percentage can be misleading and it can be more enlightening to study the behavior case by case.

The total energy is equivalent to the area under the curves in Figure 5.5. However, it is hard to distinguish any difference between the EOACC and the benchmark by eye. Another way to present the energy usage is by separating the consumed energy from the regenerated energy. The consumed, regenerated and total energy are plotted as bars in Figure 5.6 below.

For each sub-figure, the left most bar represents the consumed energy where the red bar is the benchmark's and the green is the EOACC's. The middle bar represents the regenerated energy, and the right bar represents the total energy which is the sum of the consumed and regenerated energy. Note that the axes are scaled for each sub-figure and thus the size of the bars are not comparable between sub-figures.

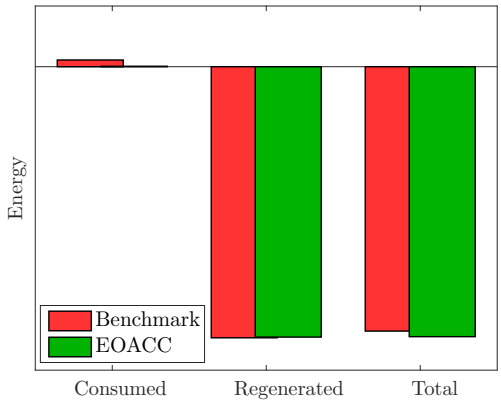

(a) Scenario 100-40 kph (1)

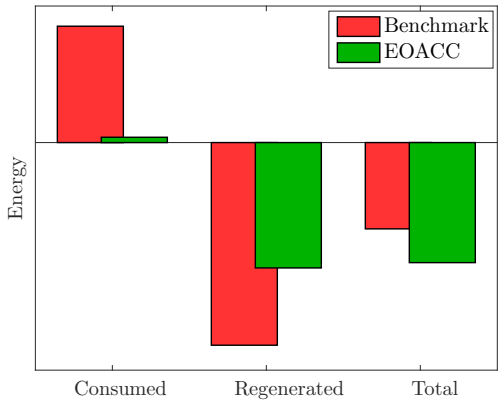

(b) Scenario 100-40 kph (2)

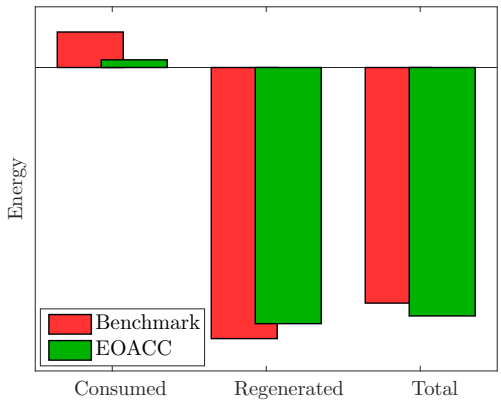

(c) Scenario 100-40 kph (3)

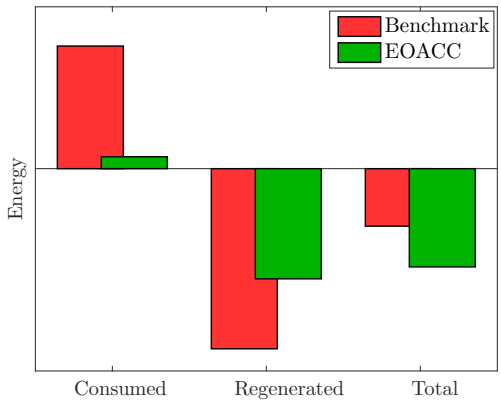

(d) Scenario 100-40 kph (4)

Figure 5.6: Consumed, regenerated and total energy for the $100-40$ kph scenarios

In the first sub-figure 5.6a, the total energy comsuption does not differ greatly. Although, the benchmark is consuming a small amount of energy which the EOACC does not resulting in an overall energy improvement.

For scenario (2), the benchmark is regenerating a larger amount of energy than the EOACC. However, it also consumes more energy. As a result, the EOACC is rewarded for not decelerating as fast as the benchmark. The plot visualizes that coasting, i.e. less regenerated energy, is favorable as energy is not required later to keep up with the target vehicle. The behavior is similar in scenario (3) and (4). Notably, without the regenerating braking, the total energy would only be the consumed energy and all energy used to brake would be wasted which makes coasting even more favorable.

5.2.2 Scenarios 60-40 kph

In this section, all four scenarios for the velocities $60-40$ kph are presented, see row $5-8$ in table 5.3. The section includes the plots of the host's velocity profiles, and how that affect the energy usage during the scenarios. The results are compared to the benchmark's results which are also presented in all plots.

Below in Figure 5.7 are plots showing the velocity profiles of the four different scenarios within the $60-40$ kph case. The green line represents the EOACC vehicle, while the red dashed line represents the benchmark.

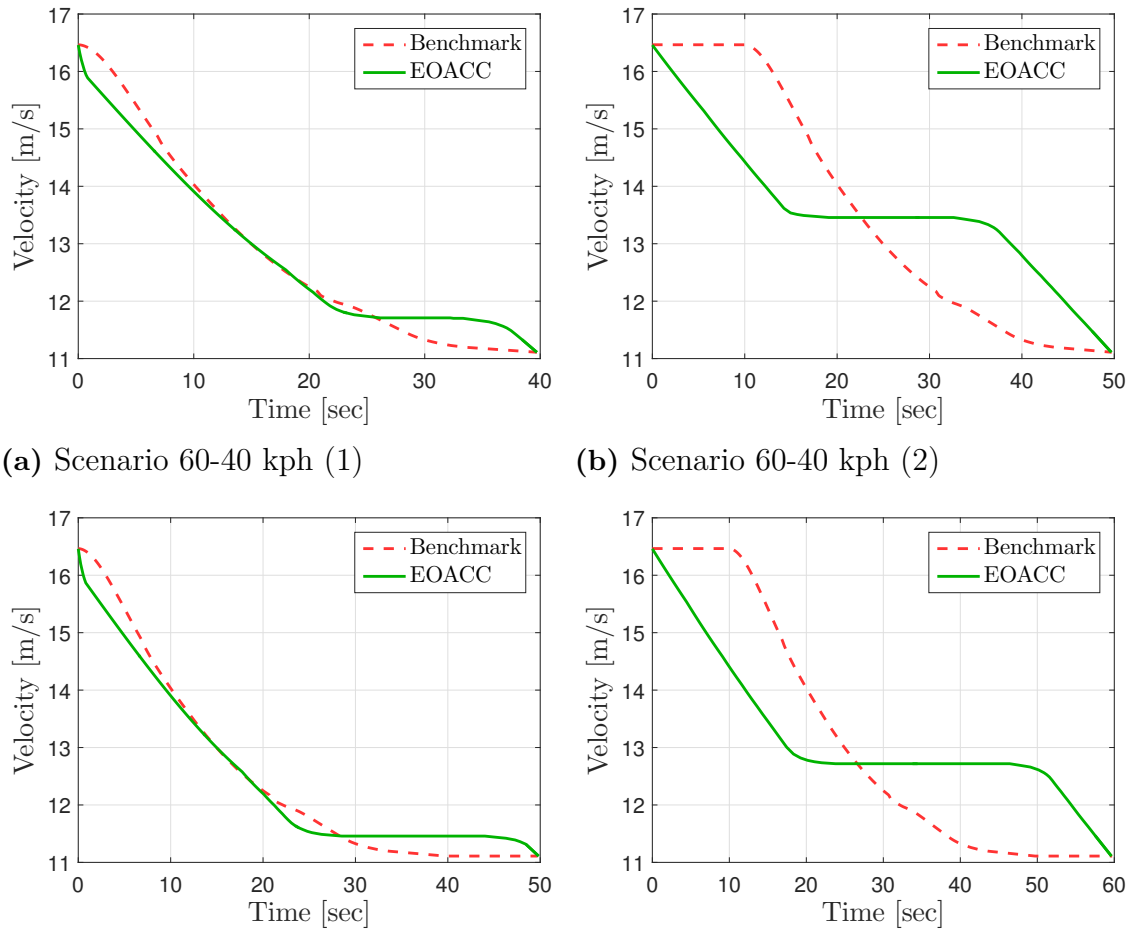

(a) Scenario 60-40 kph (1)

(b) Scenario 60-40 kph (2)

(c) Scenario 60-40 kph (3)

(d) Scenario 60-40 kph (4)

Figure 5.7: Velocity plots for all tested $60-40$ kph scenarios

Scenario (1) can be found in Figure 5.7a. The initial distance gap is 87 meter and the maneuver takes 40 seconds. The reason for the much longer maneuver time compared to the $100-40$ kph case is because the relative speed is much lower. Therefore, it takes a longer time to catch up to the target vehicle. Scenario (1) resulted in an improvement of 1.98%

The behavior in scenario (1) follows the same principle that is discussed for $100-40$ kph scenario (1). In short, the energy losses are quadratic in regard to velocity and to keep the same average velocity as the benchmark, it is beneficial to lower the speed initially while driving slightly faster near the end.

Scenario (2) has a total time of 50 seconds and the 10 extra seconds is added to the beginning when the speed is 60 kph. The extra seconds make the EOACC adapt to the target vehicle at a distance gap of 141 meters instead of 87 meters. This resulted in an improvement of 5.00%.

Scenario (3) is having a total time of 50 seconds where the 10 extra seconds were added as additional time to reach the final state. This makes the room for improvement much smaller than for scenario (2) since the extra seconds are added at the speed of 40 kph, lowering the average velocity. Scenario (3) resulted in an energy saving of 0.77%.

Scenario (4) is when 10 extra seconds were added both to the beginning and to the end. This resulted in an improvement of 4.43 %. This is the largest improvement, not in percentage, but in amount of energy, which is expected.

In contrast to the $100-40$ kph scenarios, a speed plateau, i.e. period of constant speed that is not equal to the initial or goal velocity, exists in all four scenarios with the EOACC. Since the start velocity, 60 kph, is much lower than 100 kph, it is not enough to reach the final state by only coasting. A certain relative velocity will be optimal with regard to energy per caught up distance. Therefore, we will see a plateau in the velocity curve at this specific velocity for scenarios where the vehicle can't catch up by only coasting.

E.g. if the host vehicle has a velocity of 40.1 kph while the target vehicle has a velocity of 40 kph, the energy per driven meter compared to the ground is relatively low. However, the energy required for closing in one meter on the target vehicle is comparably high since it takes a long time. Increasing the speed of the host vehicle by 1 kph in this case would barely increase the energy per driven meter compared to the ground. It would however massively decrease the energy required for closing in one meter.

The opposite would be to drive fast, e.g. 100 kph. Increasing the velocity at 100 kph by 1 kph would noticeably increase the energy per driven meter compared to the ground due to the losses being quadratically proportional to the velocity. At the same time the relative velocity would not drastically increase as for the previous case. In this case it would instead be beneficial to the decrease the velocity.

Somewhere in between, the trade-off between higher energy required due to higher velocity and lower energy required due to shorter amount of time necessary to catch up, is optimal. However, as notable in Figure 5.7, the plateau is different between the scenarios. This is because the time is punished differently to reach the specified end times.

To see where energy is saved during the scenario and whether any specific behaviors

can be identified as energy efficient or inefficient, the power is plotted in Figure 5.8 below.

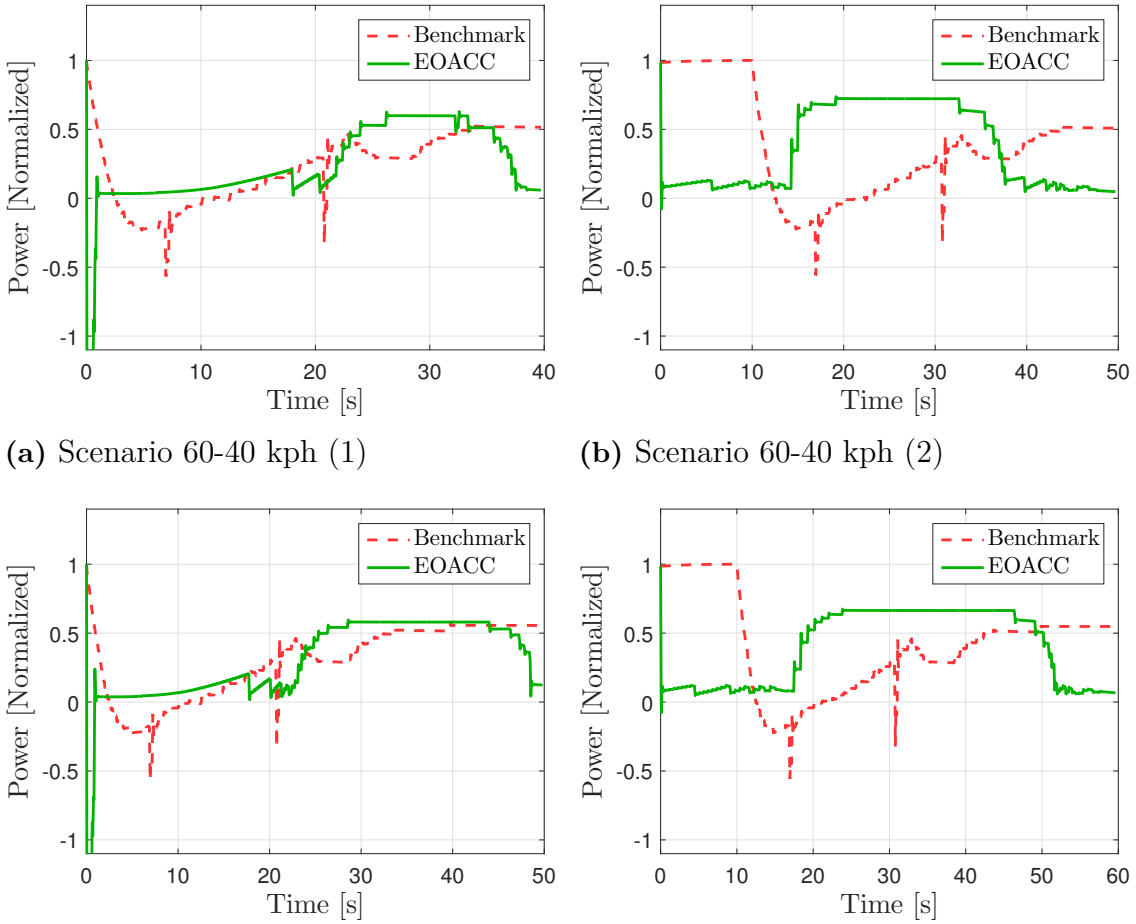

(a) Scenario 60-40 kph (1)

(b) Scenario 60-40 kph (2)

(c) Scenario 60-40 kph (3)

(d) Scenario 60-40 kph (4)

Figure 5.8: Energy plots for all tested $60 - 40$ kph scenarios

Figure 5.8 shows how the power used in every time step differs between the benchmark and the EOACC. It is not obvious by looking at the plots that the EOACC, has a lower energy consumption compared to the benchmark.

The scenarios have periods where the power is kept at slightly above zero Watt. It is not obvious why the result does not yield perfect coasting as for the $100 - 40$ kph case. A theory for scenario (1) and (3) is that coasting would yield a higher average velocity than the benchmark and thus it decelerates faster than coasting at the very beginning. For scenario (2) and (4), it seems favorable to add a small forward torque to the motor while decelerating instead of simply coasting in order to reduce the plateau.

For scenario (1), (2), (3), and (4) the savings were 1.98 %, 5.00 %, 0.77 %, and 4.43 % respectively as seen in table 5.3. As already discussed for the $100-40$ kph scenarios, the energy percentages can be misleading. Even though one scenario might have the

largest percentage, it is not necessarily the largest energy improvement. If the total energy is close to zero, a small energy improvement will yield a large percentage.

To avoid using percentages, another way to present the energy is by separating the consumed, regenerated and total energy. Below in Figure 5.9 are multiple bar plots where for each scenario, the consumed, regenerated and total energy are represented as separate bars. This makes the results easier to interpret and in turn the analysis easier.

To the far left of each sub-figure is the consumed energy where the red bar is the benchmark's consumption and the green is the EOACC. The middle bar represents the regenerated energy, and to the far right is the bar that represents the total consumed or regenerated energy. The total energy is the sum of the consumed and the regenerated energy.

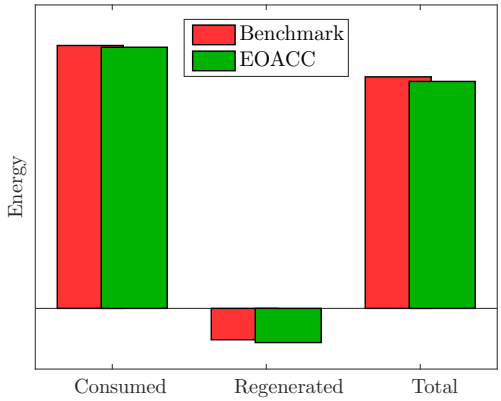

(a) Scenario 60-40 kph (1)

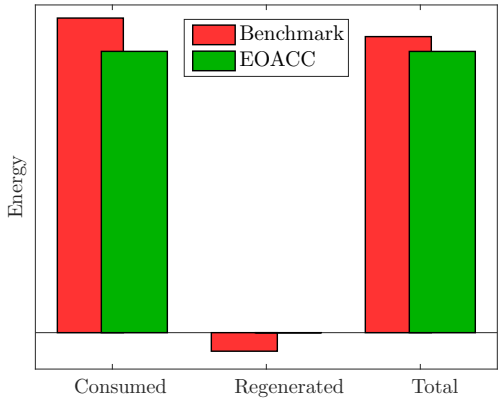

(b) Scenario 60-40 kph (2)

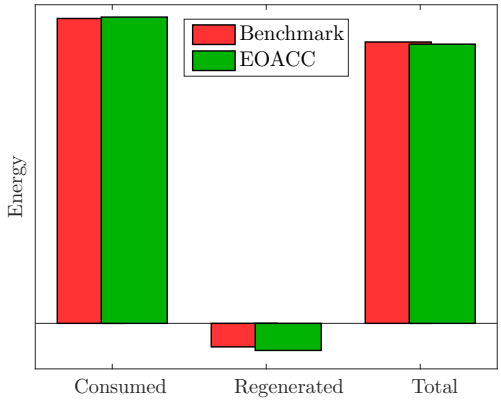

(c) Scenario 60-40 kph (3)

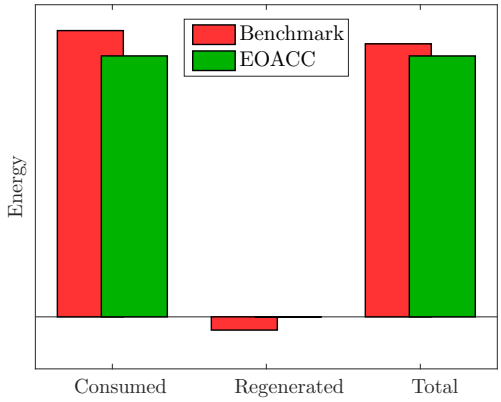

(d) Scenario 60-40 kph (4)

Figure 5.9: Consumed, regenerated and total energy for the $60-40$ kph scenarios

In sub-figure 5.9a you find the original deceleration case for $60-40$ kph. For scenario (2) and (4), the EOACC is not regenerating much energy. The main reason being that enough deceleration is generated through drag and rolling resistances alone. It

is expected that the regenerated energy is nonexistent for scenario (2) and (4) since the host vehicle can't reach the goal state by simply coasting and forward torque is required.

Scenario (1) and (3) does however regenerate some energy, although a small amount and the EOACC actually regenerates slightly more. As mentioned earlier in this section, the EOACC decelerates fairly sharply in the beginning of the scenario which yields some regeneration. Note that the deceleration still is within the allowed interval of -3.5 and 2 m/s^2 according to the ISO standard, [5].

In all four cases, it is obvious that the total amount of energy used is always less for the EOACC, however, the difference is less significant than for the $100 - 40$ scenarios. It is however a more common scenario in actual traffic and thus the results are promising.

5.3 Energy versus Time Trade-off

This thesis has focused on energy optimized solutions but always had time as equality constraints in order to obtain comparable solutions. To further explain how the time constraints affect the outcome, a time optimized and an energy optimized solution will be compared.

A velocity change from 100 to 40 kph is used to compare the behavior of the different strategies. The initial distance gap is defined to be 218 meters with an end gap of 18 meter. The scenario is similar to scenario (3) of the $100-40$ case but given more time to perform the maneuver. Below are the start and end states.

$$x_{start} = \begin{bmatrix} v_{start} \\ d_{start} \end{bmatrix} = \begin{bmatrix} 100 \\ 218 \end{bmatrix}$$

$$x_{end} = \begin{bmatrix} v_{end} \\ d_{end} \end{bmatrix} = \begin{bmatrix} 40 \\ 18 \end{bmatrix} \text{ where } v \text{ is measured in kph and } d \text{ is measured in meter.}$$

Below you find the velocity of the host vehicle for the two strategies. The time optimized strategy is displayed with an orange dashed line while the energy optimized strategy is having a green solid line. The maximum time to reach the goal state is set to be 45 seconds.

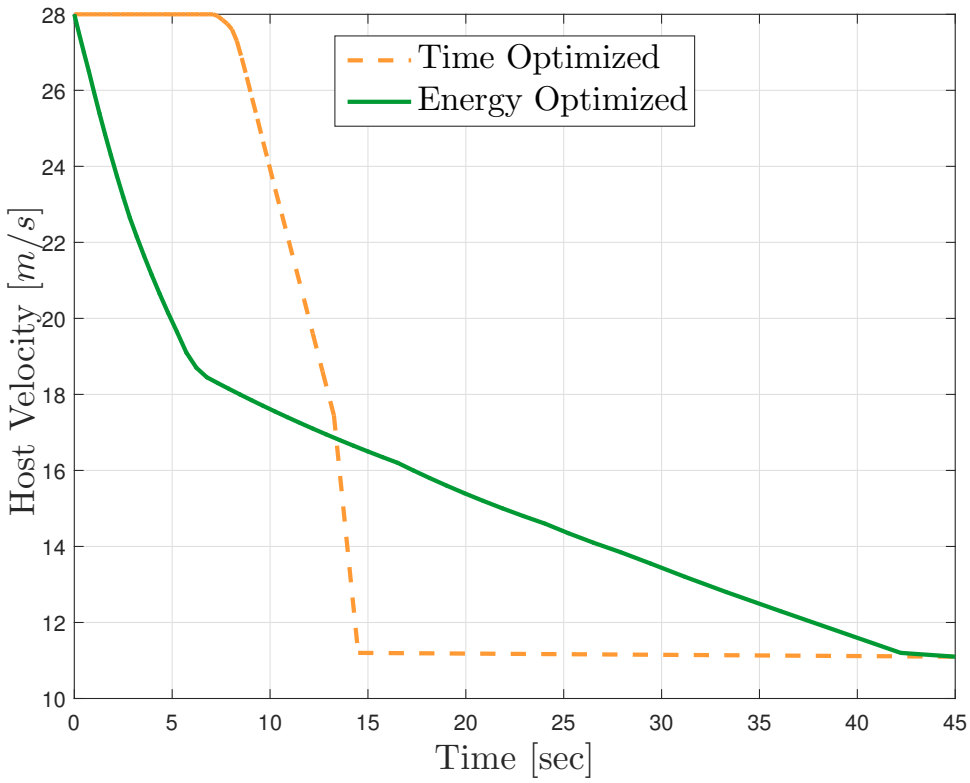

Figure 5.10: Velocity curves for a time and energy optimized strategy

Figure 5.10 shows how the time and energy optimized solution differ. The total time is decided to be 45 seconds for both solutions. This means that if the vehicle reaches the end state, x_{end}, before 45 seconds, the end velocity, 40 kph will be held for the rest of the time. This can easily be seen in Figure 5.10 as the orange curve goes down to 40 kph (11.1 m/s in the Figure) after just 15 seconds and then keeps that speed for approximately 30 seconds.

When time is minimized, the ACC wants to reach its end state as fast as possible as we saw in the Figure above. A consequence of having a distance gap as a goal, is that in order to reach the goal state, the initial speed of 100 kph is kept for as long as possible. As a result, the deceleration will saturate the amount of regenerated energy and the friction brakes convert the remaining kinetic energy to heat.

The energy optimized solution will start decelerating directly unlike the time optimized. The deceleration then merges into coasting for the rest of the scenario. That the vehicle is in fact coasting can be seen in Figure 5.11, where during coasting the total power is zero. If the maximum time of 45 seconds were longer, we would see a longer coasting period.

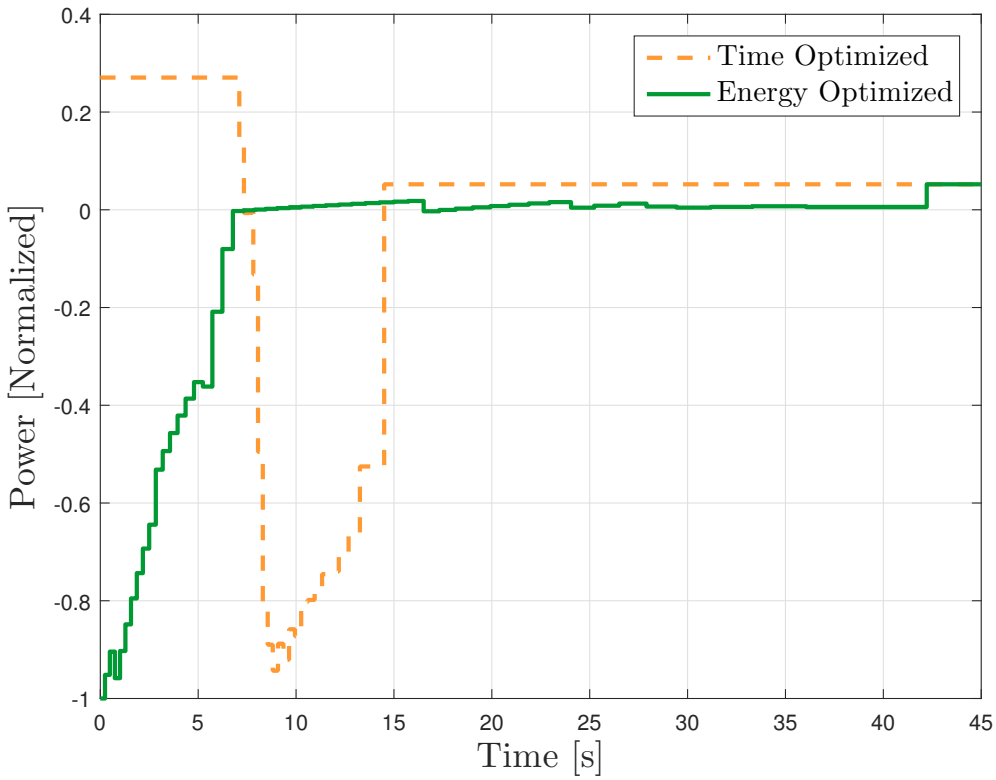

Figure 5.11: Power used for a time and energy optimized strategy

As can be seen in Figure 5.11, the power for the time optimized strategy will both have positive and negative values which means that it will both consume and regenerate energy. The energy is consumed while keeping the initial velocity for 7 seconds and while keeping the final velocity for approximately 30 seconds. The energy optimized solution on the other hand does not consume almost any energy and is mostly either coasting or regenerating energy. It is therefore avoiding all losses associated with consuming energy.

In summary, these two strategies act completely differently and is the total opposite of each other. Although, a balance of these strategies has been used in order to form the solutions presented in the thesis based on the wanted outcome.

5.3.1 Pareto Fronts

5.3 Energy versus Time Trade-off described how the energy and the time optimized strategies differ. This section examines the trade-off to see solutions between the two extremes. This was visualized by creating Pareto fronts.

This section is presenting the Pareto fronts for both the $100 - 40$ and $60 - 40$ kph scenarios. The Pareto fronts are describing the trade-off between minimizing the energy usage and minimizing the time to reach the goal state. A specific end time is predetermined in order to compare all cases. If a specific trajectory reaches the goal state after 10 seconds while another reaches the goal state after 100 seconds, those are only comparable over a period of 100 seconds or more. Thus, for the 10 second trajectory, 90 additional seconds where the vehicle maintains the goal velocity must be added. By testing the same scenario with different constraint, a Pareto front can be created where the total energy can be plotted against the time to reach the goal state.

Running enough full simulations to create a Pareto front would be very time consuming which is why the front was created by the cost function and not by the BEV model. As discussed when analyzing the cost function in section *5.1 Cost Function*, there is a consistent error estimating the energy lower than it actually is. Hence, the benchmark had to be estimated through the cost function as well to avoid any misleading results.

The Pareto fronts are based on the assumption that the EOACC trajectory and Benchmark trajectory begin to react to the target vehicle at the same time. Therefore the difference between the values of the EOACC on the Pareto front are only due to different constraints on the total time. This is similar to how scenario (1) and (3) are the same with the only difference being the total time constraint. Scenario (3) is simply scenario (1) given 10 extra seconds.

5.3.1.1 Scenarios 100-40 kph

The Pareto front presented in this section is based on the original deceleration profile from scenario (1), $100-40$ kph, see sub-figure 5.4a. The Pareto Front of the $100-40$ case is presented in Figure 5.12. The end time used for this case is 35 seconds as the energy improvement beyond this point is negligible as discussed below.

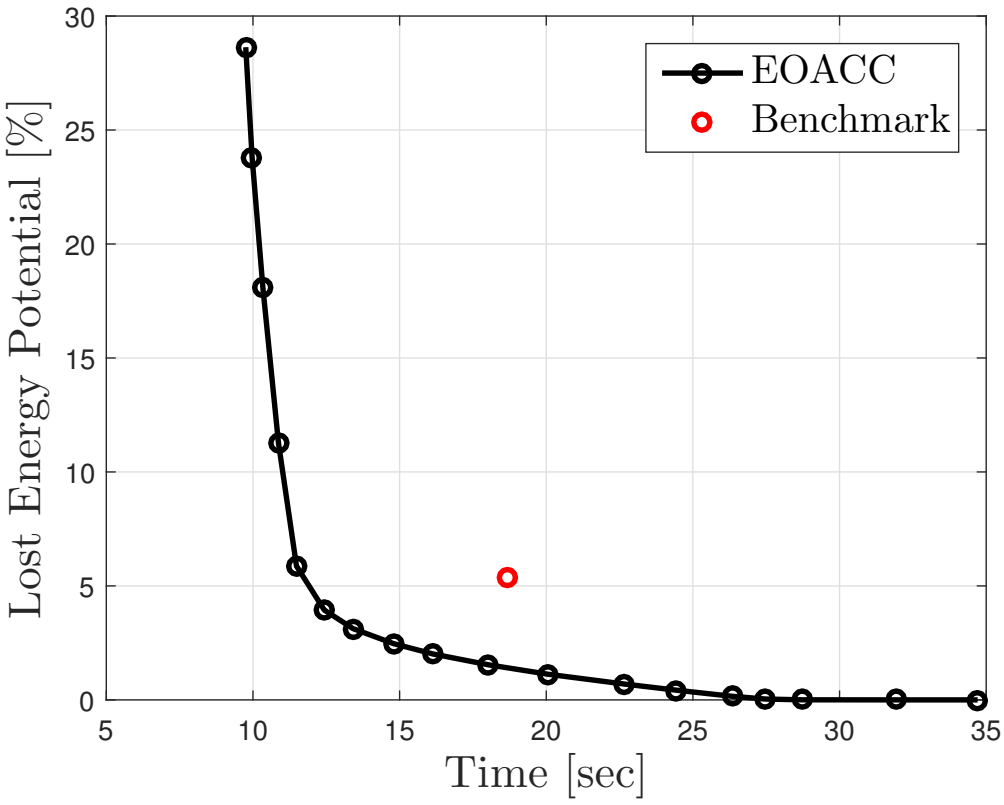

Figure 5.12: Pareto front of scenario 100-40 kph from EOACC

The x-axis represents the time to reach the goal state, that is a specific velocity and a specific time gap. The y-axis represents the lost energy potential in comparison to the best possible solution. In other words, a solution on the 20 % line could be improved by 20 % in regard to energy given more time and a different trajectory. The black line is the actual Pareto Front, where each marker is a tested scenario. The different trajectories are achieved by changing the Lagrangian multiplier λ, which essentially changes the time constraint to reach the goal state.

The Pareto front is created such that the best possible solutions given a time constraint, are along the black line, and non-optimal solutions are in the area above the front itself. It is evident that the benchmark solution, marked as red in the Figure, is not optimal. A trajectory with the same time constraint could be improved by approximately 4 %, which is seen in the Figure as the difference between the Pareto front and the red marker at the specific time. Given extra time to reach the goal state, the solution could be improved by a total of $5-6$ %. If time is prioritized, the solution could, given the same energy, be reduced to around 12 seconds compared to the current 19.

Notable from the Figure is that for this specific scenario, every second above around 27 seconds gives negligible improvements to energy. On the other end, every second below around 12 seconds is heavily punished in regard to energy.

5.3.1.2 Scenarios 60-40 kph

This Pareto front is based on the original deceleration profile from scenario (1), $60-40$, see Figure 5.7a. The end time is set to 60 seconds and the Pareto front can be seen in Figure 5.13.

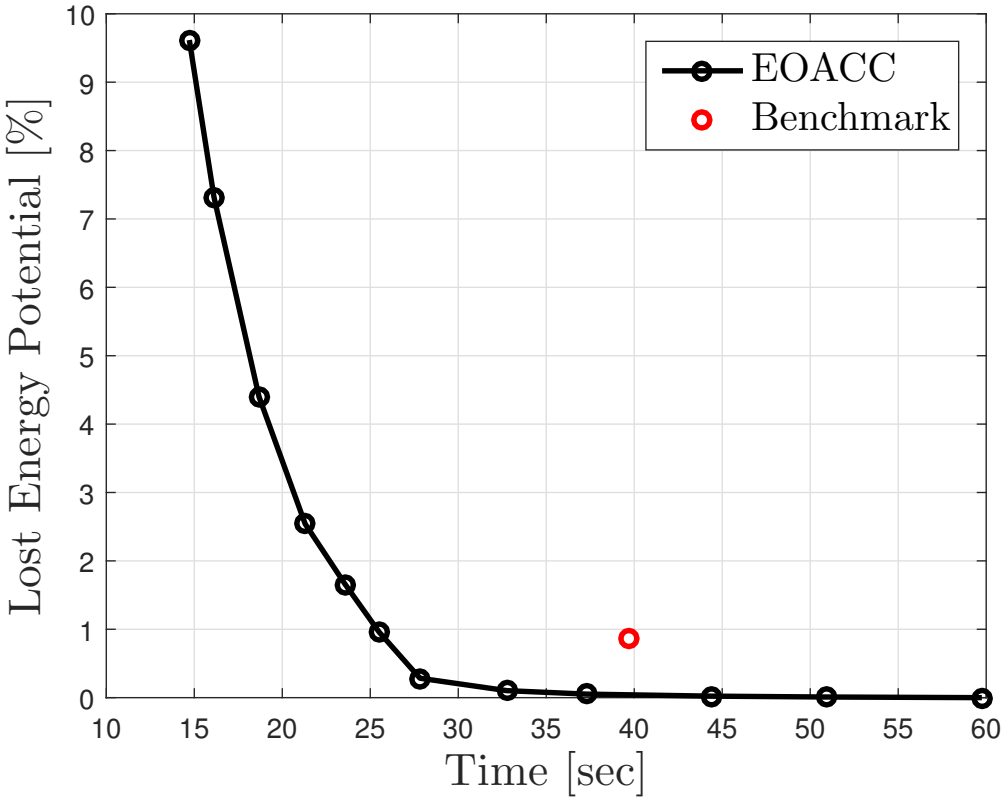

Figure 5.13: Pareto front of scenario 60-40 kph from EOACC

As for the Pareto front of the $100-40$ scenario, the black line represents the front where each marker is a tested trajectory with a different time constraint. Every solution on the front is considered optimal given the specific time constraint and every solution above the front is non-optimal.

The red marker in the Figure represents the benchmark solution. As it is above the front it is not optimal, and a different trajectory given the same time could achieve an improvement of almost 1 %. More interestingly in this case is that instead of improving the energy, the time to reach the goal state, given the same energy, could be decreased to 26 seconds from of the original 40.

As we can see in Figure 5.13, after a around 35 seconds, there is no reason to take longer time to reach the goal state. Every second beyond 35 seconds has negligible improvements to energy. On the other end, the energy required increases sharply below approximately 20 seconds.

6

Conclusion

This chapter consists of conclusions from the result chapter as well as answering the research questions stated in methodology section *4.1 Research Questions*.

The research questions we wanted to answer in this thesis were

1. What would the energy savings be for the specific traffic situations tested?

2. Is it worthwhile to optimize ACC functionality? If so, which aspects of the traditional ACC have the most potential to be optimized?

The first question is answered in the result table 5.3 in the result chapter. As the table shows, there is always some savings but they differ a lot in percentage from case to case. This is described in more detail in *5.2.1 Scenario 100-40 kph* and *5.2.2 Scenarios 60-40 kph* in the result chapter.

The results show that given the exact same initial and final position and velocity, as well as the same time to travel between the two, an energy optimized solution can decrease the energy usage by up to 2.1 % compared to a traditional ACC. Given longer time to reach the goal state, while not allowed to react earlier, the energy can be decreased by up to 5.5 %. If instead, the ACC is allowed to react earlier and the trajectory is energy optimized, the energy can be decreased by up to 39.1 %. Note that reacting earlier does not necessarily mean increasing the radar distance, but rather utilizing the information earlier.

As the results show that improvements are possible for all tested cases, it is evident that energy optimizing the ACC is worth looking into for car makers. It could be discussed how often the tested situations occur, however after test driving with the ACC active around Gothenburg, we would argue that deceleration scenarios similar to the ones presented in this thesis are very common.

The strategy of the EOACC and the benchmark seems completely different. The EOACC seem to favor coasting which is not the case for the benchmark. Interestingly, coasting would not just be favorable for battery electric vehicles but for vehicles with combustion engines as well. Therefore, the results does not necessarily show that it is worthwhile to optimize the functionality separately for BEV:s, but rather that it is worthwhile overall.

The traditional ACC has some weaknesses where the lack of coasting and the late adaptation are the most significant. Scenarios with 10 additional seconds to adapt has a significant impact on the energy consumption where coasting is one of the main reasons. The other being avoiding high velocities.

The largest difference is obtained from reacting earlier to the vehicle in front. The range of the radar is approximately 250 meter which would enable the vehicle to start adapting at that distance for all cases. The vehicle will, if allowed to react earlier, have time to coast in order to save energy and cause less air pollution caused by braking. However, reacting far in advance could lead to unnecessary braking as the traffic situation might change before the host vehicle catches up to the target vehicle.

A plateau behavior was evident in the EOACC trajectories of the $60-40$ case. While we did not see very significant improvements for the $60-40$ case, it is a far more common scenario to only have to decelerate slightly rather than a lot when using the ACC. It can therefore be interesting to evaluate whether the plateau behavior is something that should be implemented.

7

Discussion

Reacting earlier is where the biggest improvements can be obtained. This can be interpreted as an indication of how big of an impact the range of the radar has on energy consumption. However, the benchmark vehicle reacted at a different relative distance for the $100-40$ and $60-40$ case, of 127 and 90 meters respectively. This shows that the current ACC does not necessarily react at the maximum radar distance, or at least can react earlier in the $60-40$ case.

Saving energy by reacting early assumes that the target vehicle does not change lanes or accelerate. As the traffic situation might change, reacting prematurely might lead to unnecessary braking. On the other hand, it was noticeable from test driving that the opposite was likely as well, i.e. that the vehicle in front had to brake further to accommodate for slower traffic. In those cases, coasting early would be very beneficial. Depending on the situation, what is optimal might differ.

The ACC functionality is a balance between energy, time, and safety. The safety can not be compromised in any way and thus no experiments were done where the minimum relative distance was decreased. Allowing the vehicles to get closer would of course enable more time for coasting instead of braking. Therefore, the focus of this project has been between time and energy. However, energy efficiency does not necessarily oppose comfort since avoiding extreme acceleration and deceleration is beneficial in both cases [15].

The effect of jerk on comfort could be discussed as there are some jerk at the beginning and the end of the EOACC trajectories. This is because the jerk was hard to constrain at the initial and final states. However, if the trajectories were smoothed, the results would likely not differ very much.

7.1 Sources of Error

As the results of this paper are based on simulation, it is inevitable that some simplifications are made and that the results do not match reality with 100 percent accuracy. Fidelity of simulation comes at the cost of complexity and computation time. The models also could not be validated against a real car as the first Volvo BEV model has not yet reached the market, and thus there is no guarantee that the

models accurately reflect reality.

The BEV model is currently missing many of its controllers, most of which are largely irrelevant, air condition etc., however the engine controller is not yet fully implemented. The engine controller takes the requested torque and distributes the power over the engines. The current engine controller is a temporary simplified implementation and it is difficult to know how much this influences the results. Mainly it distributes the torque equally over both the front and rear engine as opposed to the real controller. The temporary engine controller also uses a fixed voltage of 450 V while the actual voltage may vary slightly over the scenario. Another simplification is that while the inertia of the wheels is taken into account, the inertia of the engine, transmission, and drive line are currently not.

The battery plant is not yet connected to its cooling system, however, as the scenarios are very short, it is very unlikely that this would influence the results. The battery performance also varies depending on the state of charge (SOC), however the effect is negligible in regard to energy consumption [8].

Furthermore, the BEV model does not have any active safety features, including an ACC. Thus, an ACC from a vehicle with a combustion engine was used and the resulting velocity profiles were then used as input for the BEV. Instead of manually converting the velocity profiles to torque, a driver module which converts velocity references to pedal positions was used. Naturally, there will be some deviation from the reference trajectory however the effect is negligible in our case as the deviations are very small.

The directed changes graph is created with the assumption that the changes velocity linearly between two states. This is accurate as long as the time steps are sufficiently small. A side effect is that the acceleration is discontinuous and can jump between values. The benefit is that differential equations are eliminated and the system can easily be simulated.

Bibliography

[1] EPA, United States Environmental Protection Agency (2019). "Global Greenhouse Gas Emissions Data".
Retrieved from https://www.epa.gov/ghgemissions/global-greenhouse-gas-emissions-data

[2] Volvo Cars (2019). Vision and Future. Retrieved from
https://www.volvocars.com/se/om-volvo/vision-och-framtid/detta-ar-volvo

[3] Grigoratos, T. & Martini, G. "Brake wear particle emissions: a review". Environmental Science and Pollution Research (2015) 22: 2491. Retrieved from
https://doi.org/10.1007/s11356-014-3696-8

[4] Greg Marsden, Mike McDonald, Mark Brackstrone. "Towards an understanding of adaptive cruise control". Transportation Research Part C: Emerging Technologies. (2001).
http://www.sciencedirect.com/science/article/pii/S0968090X0000022X

[5] International Organization for Standardization (2010) ISO 15622:2010 - Intelligent transport systems – Adaptive Cruise Control systems – Performance requirements and test procedures. Retrieved from
https://www.iso.org/standard/50024.html

[6] Gao, Yimin, Liping Chen, and Mehrdad Ehsani. "Investigation of the Effectiveness of Regenerative Braking for EV and HEV". SAE transactions (1999): 3184-3190. Retrieved from https://saemobilus.sae.org/content/1999-01-2910

[7] Latvala, S. Fakta om partiklar i luft (2018). Retrieved from
https://www.naturvardsverket.se/Sa-mar-miljon/Klimat-och-luft/Luftfororeningar/Partiklar/

[8] D Maamria, Kristan Gillet, Guillaume Colin, C Nouillant, Yann Chamaillard. On the use of Dynamic Programming in eco-driving cycle computation for electric vehicles. IEEE Conference on Control Applications (CCA) (2016). Retrieved from https://hal-univ-orleans.archives-ouvertes.fr/hal-01566889

[9] T. McKelvey (2019). Discrete Time Optimal Control, pdf.

[10] Bertsekas, D. P., Bertsekas, D. P., Bertsekas, D. P., Bertsekas, D. P. (1995). Dynamic programming and optimal control (Vol. 1, No. 2). Belmont, MA: Athena scientific.

[11] P. R. Kumar (2019). Dynamic Programming. Department of ECE, University of Illinois, USA. Retrived from http://cesg.tamu.edu/wp-content/uploads/2014/09/Dynamic-Programming-Chapter1.pdf

[12] R. K. Ahuja, T. L. Magnanti and J. B. Orlin. Network Flows: Theory, Algorithms, and Applications (1993).
Retrieved from https://labs.xjtudlc.com/labs/wldmt1/reading%20list/books/Algorithms%20and%20optimization/Network%20Flows%20Theory,%20Algorithms,%20and%20Applications.pdf

[13] S. Park, H. Rakha, K. Ahn, K. Moran (2011). Predictive eco-cruise control: Algorithm and potential benefits. IEEE Forum on Integrated and Sustainable Transportation Systems. Retrieved from https://ieeexplore.ieee.org/document/5973639

[14] Wei-Hsun Lee and Jiang-Yi Li, "An Eco-Driving Advisory System for Continuous Signalized Intersections by Vehicular Ad Hoc Network," Journal of Advanced Transportation (2018). Retrieved from https://doi.org/10.1155/2018/5060481

[15] Chen Chen, Xiaohua Zhao, Ying Yao, Yunlong Zhang, Jian Rong, and Xiaoming Liu, "Driver's Eco-Driving Behavior Evaluation Modeling Based on Driving Events," Journal of Advanced Transportation (2018). Retrieved from https://doi.org/10.1155/2018/9530470

[16] S. Akhegaonkar, L. Nouvelière, S. Glaser, F. Holzmann. Smart and Green ACC: Energy and Safety Optimization Strategies for EVs. IEEE TRANSACTIONS ON SYSTEMS (2018).
Retrieved from https://ieeexplore.ieee.org/stamp/stamp.jsp?arnumber=7565751

[17] Jay H. Lee. (2011). Model Predictive Control and Dynamic Programming. IEEE 11th International Conference on Control, Automation and Systems. (2011). Retrived from https://ieeexplore.ieee.org/stamp/stamp.jsp?arnumber=6106171